

1 **Review article: Terrestrial dissolved organic carbon in northern permafrost**

2 Liam Heffernan¹, Dolly N. Kothawala¹, Lars J. Tranvik¹

3

4 ¹Limnology/Department of Ecology and Genetics, Uppsala University, Norbyvägen 18D,
5 Uppsala 75236, Sweden

6

7 Correspondence email: liam.heffernan@ebc.uu.se

8

9

10

11

12

13

14

15

16

17

18

19

20

21

22 **Abstract**

23 As the permafrost region warms and permafrost soils thaw, vast stores of soil organic
24 carbon (C) become vulnerable to enhanced microbial decomposition and lateral transport into
25 aquatic ecosystems as dissolved organic carbon (DOC). The mobilization of permafrost soil C
26 can drastically alter the net northern permafrost C budget. DOC entering aquatic ecosystems
27 becomes biological available for degradation as well as other types of aquatic processing.
28 However, it currently remains unclear which landscape characteristics are most relevant to
29 consider in terms of predicting DOC concentrations entering aquatic systems from permafrost
30 regions. Here, we conducted a systematic review of 111 studies relating to, or including,
31 concentrations of DOC in terrestrial permafrost ecosystems in the northern circumpolar region
32 published between 2000 – 2022. We present a new permafrost DOC dataset consisting of 2,276
33 DOC concentrations, collected from the top 3 m in permafrost soils across the northern
34 circumpolar region. Concentrations of DOC ranged from 0.1 – 500 mg L⁻¹ (median = 41 mg L⁻¹)
35 across all permafrost zones, ecoregions, soil types, and thermal horizons. DOC concentrations
36 were greatest in the sporadic permafrost zone (101 mg L⁻¹) while lower concentrations were
37 found in the discontinuous (60 mg L⁻¹) and continuous (59 mg L⁻¹) permafrost zones. The highest
38 median DOC concentrations of 66 mg L⁻¹ and 63 mg L⁻¹ were found in coastal tundra and
39 permafrost bog ecosystems, respectively. Coastal tundra (130 mg L⁻¹), permafrost bogs (78 mg
40 L⁻¹), and permafrost wetlands (57 mg L⁻¹) had the highest DOC concentrations in the permafrost
41 lens, representing a potentially long-term store of DOC. Other than in Yedoma ecosystems, DOC
42 concentrations were found to increase following permafrost thaw and were highly constrained by
43 total dissolved nitrogen concentrations. This systematic review highlights how DOC
44 concentrations differ between organic- or mineral-rich deposits across the circumpolar
45 permafrost region and identifies coastal tundra regions as areas of potentially important DOC
46 mobilization. The quantity of permafrost-derived DOC exported laterally to aquatic ecosystems
47 is an important step for predicting its vulnerability to decomposition.

48

49 **1. Introduction**

50 Persistent freezing temperatures since the late Pleistocene and Holocene has led to the
51 accumulation and preservation of 1,460 – 1,600 Pg of organic carbon (C) in northern
52 circumpolar permafrost soils (Hugelius et al., 2014; Schuur et al., 2018). However, in recent
53 decades, there has been an amplified level of warming at high latitudes, occurring at four-times
54 the speed of the global average (Rantanen et al., 2021). This is leading to widespread and rapid
55 permafrost thawing which is predicted to continue under various future climate scenarios
56 (Olefeldt et al., 2016). Under the high C emissions representative concentration pathway
57 (RCP8.5), 90% loss of near-surface permafrost is projected to occur by 2300, with the majority
58 of loss occurring by 2100 (McGuire et al., 2018). Increasing temperatures and widespread thaw
59 exposes permafrost C to heterotrophic decomposition, potentially leading to enhanced emissions
60 of greenhouse gases to the atmosphere in the form of carbon dioxide (CO₂; Schuur et al., 2021)
61 and methane (CH₄; Turetsky et al., 2020). Additionally, previously frozen soil organic carbon
62 may be mobilized into the aquatic network as dissolved organic carbon (DOC), the quantity and
63 quality of which will likely depend on local and regional hydrology, and landscape
64 characteristics (Tank et al., 2012; Vonk et al., 2015). At high latitudes (>50°N), lakes and rivers
65 of various sizes cover 5.6% and 0.47% of the total area, respectively (Olefeldt et al., 2021), and
66 the landscape C balance at these high latitudes is highly dependent on aquatic C processing
67 (Vonk & Gustafsson, 2013). The increased leaching of recently thawed DOC from permafrost
68 soils will increase the currently estimated 25 – 36 Tg DOC year⁻¹ exported into the freshwater
69 system, and subsequently into the Arctic Ocean (Holmes et al., 2012; Raymond et al., 2007). It
70 may also lead to enhanced greenhouse gas emissions from freshwater ecosystems (Dean et al.,
71 2020). However, uncertainty remains as to which terrestrial ecosystems contain the highest
72 concentrations of DOC, laterally transport the greatest quantities of DOC, and represent the store
73 of DOC most vulnerable to mineralization.

74 Globally, DOC concentrations have been shown to vary across biomes, and spatial and
75 temporal scales (Guo et al., 2020; Langeveld et al., 2020). It has been suggested that at such
76 macro scales hydrology, climate, vegetation type, and soil type are important drivers of DOC
77 concentrations (Langeveld et al., 2020). Hydrology and climate are important factors shaping
78 ecosystem structure and function in permafrost regions (Andresen et al., 2020; Wang et al.,

79 2019), which in turn influences the spatial distribution of vegetation and soil types. Vegetation
80 type has been shown to be the most important driver of DOC concentrations in Arctic lakes
81 (Stolpmann et al., 2021). Carbon uptake by vegetation, via gross primary production, and SOC
82 stocks in the permafrost region have both been shown to vary across vegetation and soil types
83 (Ma et al., 2023; Hugelius et al., 2014). This variability across vegetation and soil types has
84 important implications for DOC production, which is associated with plant inputs (Moore &
85 Dalva, 2001) and the decomposition and solubilization of SOC due to soil microbial activity
86 (Guggenberger & Zech, 1993). In permafrost soils, the majority of this production is likely to
87 occur near the soil surface as the microbial production of DOC via input of plant-derived labile
88 substrates has been shown to decrease with depth (Hultman et al., 2015; Monteux et al., 2018;
89 Wild et al., 2016) and 65 – 70 % of the SOC store is found in the top 3 m (Hugelius et al., 2014).
90 The spatial distribution discrepancies observed in DOC concentrations from global assessment
91 efforts (Guo et al., 2020; Langeveld et al., 2020) may be reduced for the circumpolar permafrost
92 region by improving understanding of DOC concentrations in the top 3 m across ecosystem
93 types.

94 Previous studies have highlighted that the mineralization and lateral transport of DOC, i.e.,
95 mobilization, represents a source of terrestrial permafrost C that can potentially play an
96 important role in both terrestrial and aquatic biogeochemical cycles (Hugelius et al., 2020;
97 Parmentier et al., 2017; Schuur et al., 2022). However, none have quantified DOC mobilization
98 across the permafrost region. Inclusion of DOC mobilization in attempts to determine the
99 permafrost climate feedback (Schaefer et al., 2014), may reduce current uncertainty in the
100 magnitude and location of permafrost C losses (Miner et al., 2022), particularly as permafrost
101 thaws. Warming of near surface permafrost causes widespread thawing (Camill, 2005; Jorgenson
102 et al., 2006), which can lead to drastic changes in hydrology, vegetation, and soil carbon
103 dynamics (Liljedahl et al., 2016; Pries et al., 2012; Varner et al., 2022), thus impacting both
104 DOC production and mobilization. Several studies have demonstrated that DOC has the potential
105 to be rapidly degraded and mineralized following thermokarst formation (Burd et al., 2020;
106 Payandi-Rolland et al., 2020; Wickland et al., 2018), particularly in higher latitude ecosystems
107 (Ernakovich et al., 2017; Vonk et al., 2013). However, few have compared this lability across
108 ecosystems (Abbot et al., 2014; Fouche et al., 2020; Textor et al., 2019) and less have done so

109 across the permafrost region (Vonk et al., 2015). Determining the ecosystems with the greatest
110 store of DOC that is readily mineralized upon thermokarst formation represents a potentially
111 important step in reducing uncertainty in the permafrost climate feedback.

112 Here, we conduct a systematic review of the literature and compiled 111 studies published
113 between 2000 – 2022 on DOC concentrations in the top 3 m of soil in terrestrial ecosystems
114 found in the northern circumpolar permafrost region. Our aim was to build a database to assess
115 the concentration and mobilization of DOC across terrestrial permafrost ecosystems. We used
116 this database to address the following hypotheses; (i) the highest DOC concentrations would be
117 found in organic rich wetland ecosystems; (ii) disturbance would lead to increased export and
118 biodegradability of DOC; and (iii) the most biodegradable DOC would be found in Yedoma and
119 tundra ecosystems. A quantitative assessment of studies pertaining to DOC concentrations in
120 permafrost soils can identify evidence-based recommendations for future topics, standardisation
121 of methods, and areas of research to improve our understanding on terrestrial and aquatic
122 biogeochemical cycling in northern permafrost regions. Our database contains ancillary data
123 describing the geographical and ecological conditions associated with each DOC concentration,
124 allowing us to reveal patterns in DOC concentrations and lability measures for 562 sampling
125 sites across multiple ecosystem types and under varying disturbance regimes. This study
126 represents the first systematic review of DOC concentrations within terrestrial permafrost
127 ecosystems found in the circumpolar north. As such, it provides unique and valuable insights into
128 identifying ecosystems associated with the highest DOC concentrations, and thus ecosystems
129 with the greatest potential for DOC mobilization.

130 **2. Methods**

131 This systematic review used a methodological framework proposed by Arksey &
132 O'Malley (2005) and follows five steps: 1) develop research questions and a search query; 2)
133 identify relevant studies; 3) study selection; 4) data extraction; and 5) data analysis, summary,
134 and reporting. The literature search was guided by four research questions: 1) what are the
135 concentrations of DOC found in terrestrial ecosystems across the northern circumpolar
136 permafrost region?; 2) what are the rates of export and/or degradation (mobilization) of DOC
137 within these ecosystems?; 3) What are the major controls on DOC concentrations and rates of
138 mobilization?; and 4) how are concentrations and mobilization rates impacted by thermokarst

139 formation? Mobilization rates represent DOC loss and include specific discharge of DOC (g
 140 DOC m⁻²), export rate of DOC per day (g C m⁻² day⁻¹) and per year (g C m⁻² year⁻¹), and
 141 biodegradable DOC (BDOC; %).

142 *2.1 Literature Search*

143 Based on *a priori* tests, we used the following search query string to find papers using
 144 information found in their title, abstract, and keywords: ("dissolved organic carbon") AND
 145 (permafrost OR thermokarst OR "thaw slump") AND (soil OR peat) AND (export OR degrad*
 146 OR decomposition OR mineralization). We used Web of Science, Science Direct, Scopus,
 147 PubMed, and Google Scholar to generate a database of tier 1, peer-reviewed articles published
 148 between 2000 – 2022. The search function on Science Direct does not support the use of
 149 wildcards such as "*", so "degrad*" was changed to "degradation". We removed duplicate
 150 references found across multiple databases using Mendeley© referencing software (v1.17.1,
 151 Mendeley Ltd. 2016). We used the same search query string as above to search for articles on the
 152 first 15 pages of Google Scholar. This resulted in the addition of a further 150 articles to be
 153 included in our systematic screening process.

154 *2.2 Systematic Screening of Peer-Reviewed Publications*

155 The selection of relevant studies was comprised of inclusion criteria and relevance
 156 screening in three steps. In the first step we placed limits on initial study searches in the
 157 electronic databases mentioned above. Studies were included in the review if they were primary
 158 research, published in English, and published between 2000 – 2022 (Table 1). Only quantitative
 159 studies conducted in terrestrial ecosystems within the northern circumpolar permafrost region, as
 160 defined by Brown et al., (1997), and reporting DOC concentration and mobilization rates were
 161 included. Studies not meeting these criteria were eliminated and the remaining studies proceeded
 162 to the second screening step.

Table 1. Summary of criteria used to identify suitable studies in the preliminary screening stage

	Inclusion criteria	Exclusion criteria
Timeline	Study published between 2000 – 2022	Study published prior to 2000

Study type	Primary research article published in peer-reviewed journal using quantitative methods	Thesis/dissertations and secondary research studies (reviews, commentaries, editorials)
Language	Published in English	Studies published in other languages
Region	Conducted within the northern circumpolar permafrost region	Conducted outside of the northern circumpolar permafrost region
Outcome	Studies on DOC concentration, export or degradation in permafrost environments	Studies not on DOC concentration, export or degradation in permafrost environments

163

164 In the second step, the primary relevance of articles was screened, based on article titles,
165 abstracts, and keywords, and the eligibility criteria provided in Table 2. Studies deemed
166 irrelevant were eliminated and the remaining studies proceeded to the third and final screening
167 step, or secondary screening stage, which was based on was based on more specific eligibility
168 criteria (Table 2) applied to the full text.

Table 2. Primary and secondary relevance screening tools. Primary screening tool used in the article title, abstract, and keyword screening stage. Secondary screening tool used in full-text screening stage

Screening stage	Screening questions	Response details
Primary	Does the study involve quantitative data collected from a permafrost environment?	Yes – reports on quantitative data collected from a permafrost environment No – does not report on the above
Primary and Secondary	Is the study region within the northern circumpolar permafrost region?	Yes – reports on quantitative data (including field observations and lab data) collected from the circumpolar permafrost environment. No – study region is not in the northern circumpolar permafrost regions; other examples could be mountainous permafrost or Tibetan plateau
Primary and Secondary	Is the article in English and NOT a review, book chapter, commentary, correspondence,	Yes – study is in English and is a primary research article that includes quantitative studies (field and lab based), including model-based research as it relies on observational data.*

	letter, editorial, case report, or reflection?	No – study is not in English and/or is a review, book, editorial, working paper, commentary, conference proceeding, supplementary text, or qualitative study which does not address outcomes relevant to this review
Primary and Secondary	Does the study involve the concentration, export or degradation of terrestrially derived DOC?	Yes – reports on terrestrial DOC concentration, export, or degradation, including concentrations and characterization No – does not report on terrestrial DOC concentration, export, or degradation
Secondary	Is the article in English, longer than 500 words, and published between 2000 - 2022?	Yes – study is published between 2000 – 2022 No – study is published prior to 2000

169 *For model-based studies, the original field/lab data used to parametrise or develop the model
170 was used. If this data was taken from previously published work, then those studies were used
171 and the model-based study removed.

172 *2.3 Database compilation*

173 A database with reported DOC concentrations and mobilization rates i.e., rates of either
174 DOC export or degradation, was compiled using data from all studies that were deemed relevant
175 following the study selection phase. The database was compiled to compare DOC concentrations
176 and mobilization rates between different sites. We define a site as an area where either soil,
177 water, or ice samples were taken from that has similar vegetation composition, water table
178 position, permafrost regime, and was either disturbed or pristine. Site descriptions were derived
179 from the text of each study. Where possible, individual daily measurements of DOC
180 concentrations and mobilization rates were taken. When replicates of the same daily
181 measurement were provided, we used the mean of those replicates, which was relevant for 10
182 studies within the database, representing 72 DOC concentrations. All data was extracted from
183 data tables, text, supplementary material, or extracted from data figures using WebPlotDigitizer
184 (<https://automeris.io/WebPlotDigitizer>).

185 All studies reported measuring DOC concentrations collected from either open-water, pore
186 water, ice, or soil using a median filter pore size of 0.45 μm with first and third quartiles pore
187 size of 0.45 and 0.7 μm . Measurements from all 12 months of the year were included in the

188 database with the majority occurring during the growing season (May – August), a small portion
189 during the non-growing season, and the remaining sampling times were either not reported or are
190 averages over multiple sampling occasions. We included data from studies that were both field
191 and lab based. However, any data where a treatment was applied was excluded, except for
192 temperature treatments during incubation experiments when assessing the biodegradability of
193 DOC. When lab-based studies included an incubation, only Day 0 DOC concentrations were
194 used when comparing DOC concentrations across studies. We chose to remove any DOC
195 concentrations from samples taken below 3 m depth, which represented 3% of all DOC
196 measurements. These measurements were removed for better comparability with the current best
197 estimation of soil organic carbon stocks within the northern circumpolar permafrost zone
198 (Hugelius et al., 2014). We also removed any DOC concentrations greater than 500 mg L⁻¹,
199 which represented 2% of all DOC concentrations. Samples that were above 500 mg L⁻¹ and were
200 sampled below 3 m represented 1% of all DOC concentrations.

201 Site averaged daily DOC concentrations (mg L⁻¹) and mobilization rates were estimated from
202 the average concentration and mobilization rates measured within a single day or sampling
203 occasion. Repeated measurements at a site, either over the growing season or multiyear
204 measurements, were treated as an individual estimate of DOC concentrations and mobilization
205 rates. Other continuous variables that were similarly estimated include soil moisture, water table
206 position, organic layer depth, active layer depth, bulk density of soil, soil carbon content (%),
207 soil nitrogen content (%), carbon:nitrogen, pH, electrical conductivity (μS cm⁻¹), specific UV
208 absorbance at 254 nm (SUVA; L mg C⁻¹ m⁻¹), total dissolved nitrogen (mg L⁻¹), nitrate (mg L⁻¹),
209 ammonium (mg L⁻¹), chloride (mg L⁻¹), calcium (mg L⁻¹), and magnesium (mg L⁻¹). The
210 aromatic content of organic matter is positively correlated with SUVA (Weishaar et al., 2003),
211 with high SUVA values being used as an indication of high aromatic content (Hansen et al.,
212 2016). Ratios of C:N have been shown to be a good proxy for decomposition (Biester et al.,
213 2014), where high C:N values indicate higher decomposition. Mean annual temperatures and
214 precipitation, sampling depth, filter size, the number of days over which sampling took place,
215 how many years following disturbance measurements were taken were also recorded. Several
216 continuous variables other than those mentioned above were also recorded in the database, but
217 not used for analysis if they represented < 20% of the database. We chose 20% as the cut-off

218 point for use in comparison of the relationship between DOC concentrations and mobilization
219 with other site continuous variables.

220 Categorical variables included in the database were site location within the permafrost zone
221 (continuous, discontinuous, sporadic; Brown et al., 1997) and ecoregion (arctic tundra, sub-arctic
222 tundra, sub-arctic boreal, and continental boreal; Olson et al., 2001). We included site surface
223 permafrost conditions (present or absent), the thermal horizon layer sampled (active layer,
224 permafrost, permafrost free, water, and thaw stream), and if present what type of disturbance
225 occurred at the site (fire, active layer thickening, thermokarst terrestrial, or thermokarst aquatic).
226 Active layer represents the seasonally unfrozen soil layer above the permafrost layer. Permafrost
227 Lens represents the permanently frozen (below 0 °C) layer. Permafrost lens DOC concentrations
228 are determined from soil and pore water within the permafrost layer and extracted via frozen
229 cores, whereas active layer samples are taken from soil cores or porewater that are unfrozen at
230 the time of sampling. Thaw Stream represents flowing surface waters following permafrost thaw.
231 Permafrost Free represents areas that are not underlain by permafrost. We also included the soil
232 class found at the site (Histel, Histosol, Orthel, and Turbel; USDA, 1999) and whether the DOC
233 was from the organic or mineral soil. Histosols are organic rich, non-permafrost soils. Histels,
234 Orthels, and Turbels are permafrost-affected soils (Gelisol order). Histels are organic rich,
235 Orthels are non cryoturbated affected mineral soils, and Turbels are cryoturbated permafrost
236 soils. Organic rich Histel and Histosol soils have been previously shown to contain greater SOC
237 stocks in the top 3 m of soil than the mineral rich Orthel and Histel soils (Hugelius et al., 2014).
238 To assess the influence of sampling approach and method of analysis, we included method of
239 DOC extraction (centrifugation of soil sample, leaching and dry leaching of soil, dialysis, grab
240 sample, ice core extraction, potassium sulphate extraction, lysimeter, piezometer, pump, rhizons)
241 and DOC measurement method (combustion, persulphate, photometric, or solid-phase
242 extraction).

243 Sites were classified according to ecosystem type, and these included coastal tundra, forest,
244 peatland, permafrost bog, permafrost wetland, retrogressive thaw slump, upland tundra, and
245 Yedoma. Ecosystem classification is based on the general site description in the article, the
246 provided ecosystem classification within the article, and site data including vegetation
247 composition, permafrost conditions, and ecoregion. Coastal tundra sites includes typical

248 polygonal tundra features found along the coastline in the permafrost region (Lantuit et al.,
249 2012). Forests include any forested ecosystem, such as a black spruce forest (Kane et al., 2006)
250 or larch forest (Kawahigashi et al., 2011) where the soil is not a wetland soil. Peatlands are sites
251 classified as either fens (Olefeldt and Roulet 2012) or bogs (Olsrund and Christensen 2011) that
252 are within the permafrost domain but are not underlain by permafrost. Permafrost bogs are sites
253 that are bogs and are either underlain by permafrost (O'Donnel et al., 2016) or are thermokarst
254 bogs (Burd et al., 2020) that were previously underlain by permafrost prior to thawing.
255 Permafrost wetlands sites include saturated soils that are underlain by permafrost, or were
256 previously underlain by permafrost prior to permafrost thaw. They contain sampling locations
257 typical of moist acidic tundra (Trusiak et al., 2018), tundra meadows (Tanski et al., 2017), and
258 high-latitude fens (Nielsen et al., 2017). Retrogressive thaw slumps are areas where substantial
259 ground ice degradation leads to thermokarst and the resulting feature contains a retreating
260 headwall (Abbott et al., 2015). Upland tundra sites are high-latitude, non-wetland, mineral soils
261 that include tundra heath (Stutter and Billett 2003) and meadows (Hirst et al., 2022). Yedoma
262 sites include pristine forest, upland tundra, and coastal tundra, as well as retrogressive thaw
263 slumps and other thermokarst features found within the Yedoma permafrost domain (Strauss et
264 al., 2021). The ecosystem classification retrogressive thaw slump only includes these
265 thermokarst features found outside the Yedoma permafrost domain. Each ecosystem type was
266 further classified based on the type of permafrost thaw or thermokarst formation that occurred
267 there. These thaw or thermokarst types included thermokarst bog, thermokarst wetland, active
268 layer thickening, retrogressive thaw slump, exposure, thermo-erosion gully, and active layer
269 detachment.

270 *2.4 Database analysis*

271 All statistical analyses were carried out in R (Version 3.4.4, R Core Team, 2015). We aimed
272 to assess how DOC concentrations differed across study regions and ecosystems. To do this we
273 used Kruskal-Wallis analysis to test for differences in median DOC concentrations among the
274 various study regions and areas that included permafrost zones, ecoregions, soil class, thermal
275 horizon, and ecosystems. Post-hoc comparisons of median DOC concentrations among these
276 categories were performed using pairwise Wilcox test. Within and between each ecosystem type
277 we assessed the differences in DOC concentrations found in different thermal horizons (i.e.,

278 active layer and permafrost lens). To do this, data was first transformed using a Box Cox
279 transformation and the optimal λ using the *MASS* package (Ripley et al., 2019). We then
280 performed analysis of covariance (ANCOVA) to test for differences in DOC concentrations in
281 different thermal horizons between ecosystem types, while controlling for seasonal effects by
282 including the month in which sampling occurred as the covariate.

283 Following the assessment of differences in DOC concentrations across these study regions
284 and ecosystems we aimed to assess the influence of extraction and analysis method on DOC
285 concentrations. The aim of this was to determine if extraction and analysis method was having a
286 greater effect on DOC concentrations than study region or ecosystem. To do so we first used
287 ANOVAs and Bonferroni post-hoc tests on linear mixed effects models, that include either
288 extraction method, filter size, or analysis method as a fixed effect and ecosystem type as a
289 random factor, to evaluate significant differences in DOC concentrations between DOC
290 extraction and measurement methods. We then performed Kruskal-Wallis analysis to test for
291 differences in median DOC concentrations among the extraction method, filter size, and analysis
292 method in each permafrost zone, ecoregion, soil class, thermal horizon, and ecosystem. Post-hoc
293 comparisons of median DOC concentrations among these categories were performed using
294 pairwise Wilcox test.

295 We used partial least squares regression (PLS) when assessing the relationship of DOC
296 concentrations with continuous and categorical variables. We performed this analysis to
297 determine how the drivers of DOC concentrations across ecosystems may explain the variability
298 in DOC concentrations. Predictor variables were categorized based on their Variable Importance
299 in Projections (VIP) method in the *plsVarSel* package (Mehmood et al., 2012), whereby variables
300 with a score $> 0.6 - 1$ are deemed to be significant (Chong and Jun 2005). We ran several PLS
301 including predictor variables with a VIP of $> 0.6, 0.7, 0.8, 0.9,$ and 1 . The most parsimonious
302 PLS model contained predictor variables with a VIP > 1 and was selected based on the
303 proportion of variability in the predictors explained by the model, significant PLS components,
304 Q^2 , and background correlation (Andersen and Bro 2010). PLS was performed using the *pls*
305 package (Mevik & Wehrens, 2007) and we chose to use PLS as it is tolerant of co-correlation of
306 predictor variable, deviations from normality, and missing values, all of which were found within
307 the database. In the PLS ecosystem classes were subdivided into pristine or disturbed (i.e.,

308 impacted by permafrost thaw). Pristine sites were further subdivided by the thermal horizon in
309 which the DOC concentrations were measured (active layer and permafrost lens). Sites were split
310 into disturbed and pristine to assess whether disturbances has an impact on DOC concentrations.
311 Pristine sites were divided by their thermal horizon to assess whether DOC concentrations were
312 more positively related to the active layer exposed to both microbial decomposition and fresh
313 annual carbon inputs from surface vegetation, or the permafrost lens.

314 To evaluate the change in ecosystem DOC concentrations following thermokarst formation,
315 based on all studies from the systematic review, we calculated the response ratio using the
316 *SingleCaseES* package (Pustejovsky et al., 2021). We define thermokarst as the process by which
317 ice-rich permafrost deposits undergo complete thaw, resulting in surface subsidence and the
318 formation of a new, thermokarst feature that is ecological different regarding water table
319 position, redox conditions, and vegetation type, from the preceding pristine ecosystem. Very few
320 studies in our database report DOC concentrations for both pristine and thermokarst affected
321 ecosystem (< 20 %). To include as much data as possible we chose an effect size metric that is
322 unlikely to be influenced by studies with large sample number and variance. The response ratio
323 is;

$$324 \text{ Pristine to Thermokarst Effect Response ratio} = \ln\left(\frac{X_P}{X_T}\right) \quad \text{Eqn. 1}$$

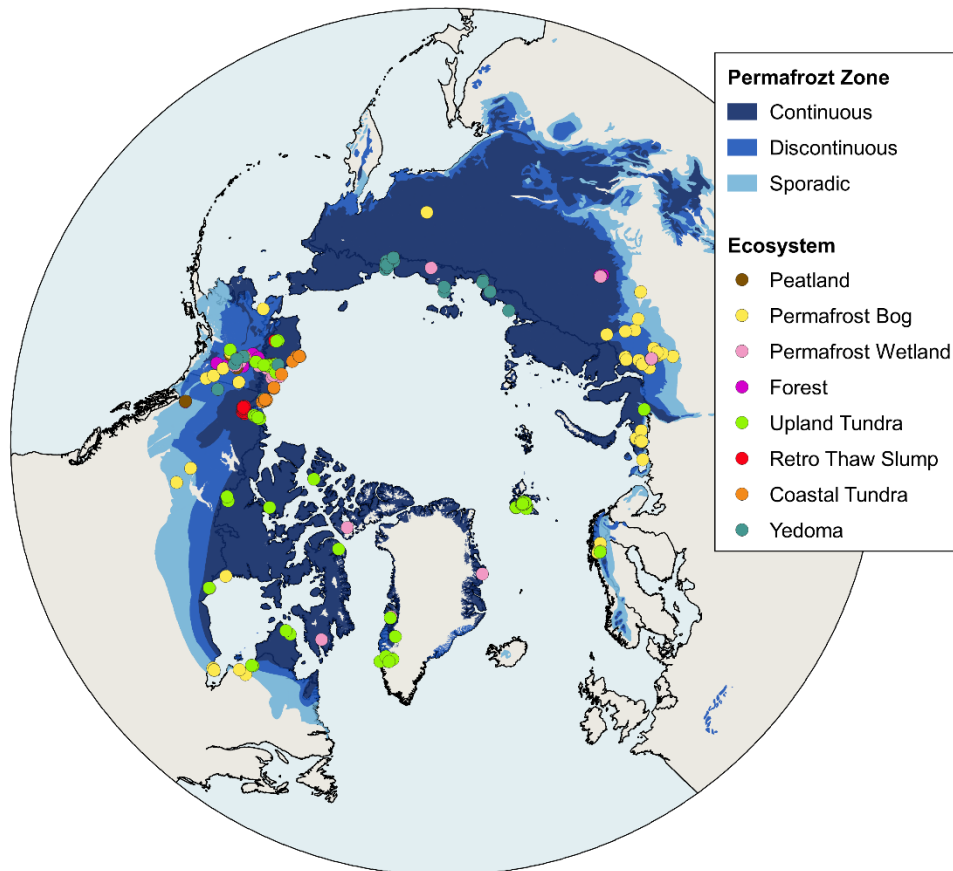
325 where X_P = mean DOC concertation of pristine ecosystems and X_T = mean DOC concertation of
326 thermokarst effected ecosystems (Lajeunesse, 2011). This represents the log proportional
327 difference in mean DOC concentrations between thermokarst and pristine ecosystems, where a
328 positive response ratio indicates a decrease in DOC concentrations following thermokarst.

329 The distribution of the data was inspected visually and with the Shapiro–Wilk test. We tested
330 homogeneity of variances using the *car* package and Levene’s test (Fox and Weisberg, 2011).
331 We report DOC concentrations as the median value with uncertainty as \pm the interquartile range,
332 except for response ratios which we report as \pm 95% confidence intervals. We here define the
333 statistical significance level at 5%.

334 **3. Results**

335 *3.1 Database generation*

336 Our initial search using Web of Knowledge, Science Direct, Scopus, PubMed, and
337 Google Scholar returned a total of 577 unique papers published between 2000 – 2022 that assess
338 the concentrations and rates of mobilization of DOC in terrestrial ecosystems within the northern
339 circumpolar permafrost region. Of these initial 577 studies, 111 remained after the systematic
340 screening process (Table 1 & 2). From these 111 studies we generated our database. The final
341 database of 111 studies contained a total of 3,340 DOC concentrations (mg L^{-1}), with 2,845 DOC
342 concentrations between 0 – 500 mg L^{-1} , found within the top 3 m of permafrost soils from field
343 and lab-based studies (using only Day 0 lab-based DOC concentrations). These concentrations
344 were taken from 562 different sampling locations, representing 8 different ecosystem types
345 (Figure 1; Table S1) across the northern circumpolar permafrost region. All studies except, for
346 one (Olefeldt et al., 2012), reported DOC concentrations.



347

348 Figure 1. Map of sampling locations where DOC measurements (n=562) from the top 3 m for
349 each ecosystem type. In many cases, the same sampling location was used in multiple studies
350 leading to some overlap, therefore the number of sampling sites included in the data set (562)
351 are not all clearly identifiable from this map. Similarly, several points overlay others even when
352 the ecosystems differ. For a full list of site coordinates please see the database (repository link).
353 Retro Thaw Slump = Retrogressive Thaw Slump. Blue shading represents permafrost zonation
354 (Brown et al., 1997).

355

356 The final database contained a considerably lower number of DOC mobilization
357 measurements. The database includes 16 measurements of specific discharge of DOC (g DOC m^{-2}
358 day^{-1}) from 3 studies, 9 export rate of DOC per day ($\text{g C m}^{-2} \text{day}^{-1}$) and per year ($\text{g C m}^{-2} \text{year}^{-1}$)
359 measurements were each found in 2 studies. The number of specific discharge, export of DOC
360 per day, and export of DOC per year measurements combined were <1% of the number of DOC
361 concentration measurements. As such they were not considered for analysis of DOC
362 mobilization. A total of 146 BDOC (%) measurements, 4% of the total number of DOC
363 concentration measurements, were found in 14 studies. These measurements of BDOC were
364 from Yedoma (30:5, number of measurements:studies), Upland Tundra (55:5), Forest (18:3),
365 Permafrost Wetland (12:2), and Permafrost Bog (31:5) ecosystems. Given the low number of
366 other forms of DOC mobilization and relatively comparable spread of BDOC measurements
367 across ecosystem types, we chose to include BDOC measurements in our analysis despite a low
368 total number of measurements compared to DOC concentrations, and we consider this lower
369 sample size during our interpretation of results.

370 Filter size used in studies ranged from 0.15 – 0.7 μm . The majority of DOC
371 concentrations reported were determined using a filter size of 0.45 μm (58%), 0.7 μm was the
372 second most common filter size (21%), followed by 0.22 μm (14%). We identified eleven
373 different DOC extraction methods in total from both soils and water that are broadly grouped
374 into the following six extraction types; leaching, suction, grab, centrifuged, dialysis, and
375 potassium sulphate (K_2SO_4) extraction. Leaching includes the leaching and dry leaching of soil;
376 suction includes lysimeter, piezometer, pump, and rhizons; grab includes grab samples and ice
377 core extraction; and centrifuged, dialysis, and (K_2SO_4) extraction remain on their own. Suction
378 (42%), leaching (37%), and grab (14%) were the three most common extraction methods across
379 all samples. Leaching and suction extraction methods were used for 66% and 24%, respectively,

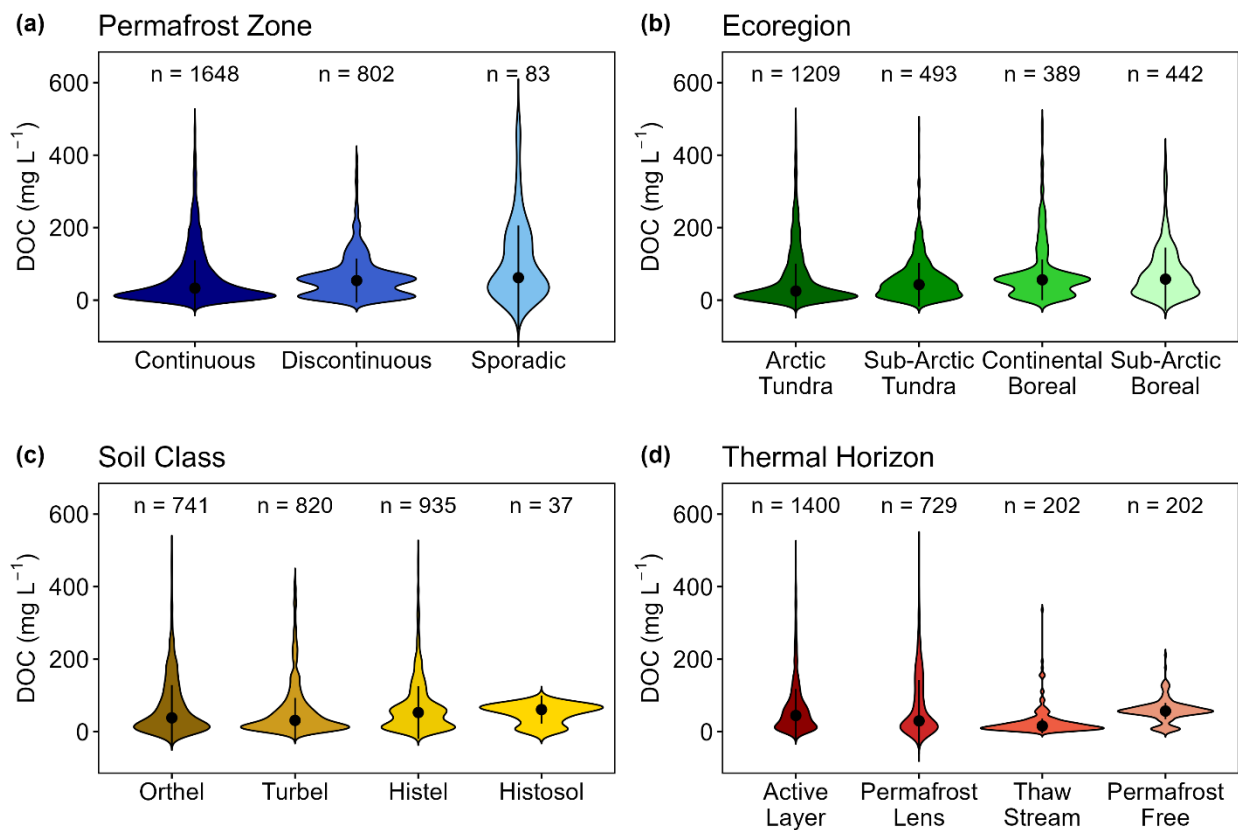
380 for all soil samples. For water samples, suction (65%) and grab (31%) were the most common
381 extraction methods. The most common measurement method to determine DOC concentrations
382 was by the combustion method (89%), followed by the persulphate (9%) and photometric (1%)
383 methods.

384 3.2 DOC concentrations and study regions

385 Upon inspection of DOC concentrations in the database, we determined that the data was
386 non-normally distributed. The DOC concentrations were skewed toward the lower end of our 0 –
387 500 mg L⁻¹ range; thus, we report median, upper, and lower quartiles below. Across all studies,
388 within the top 3 m of soil, the median DOC concentration was 41 ± 74 mg L⁻¹. DOC
389 concentrations were found to differ among the three permafrost zones (chi-square = 32, df = 2, *p*
390 < 0.001; Figure 2a). The highest median DOC concentrations were found within the sporadic
391 permafrost zone (n = 83; 62 ± 144 mg L⁻¹). The lowest median of 33 ± 77 mg L⁻¹ was found in
392 the continuous permafrost zone (n = 1,648), with the greatest density of samples having lower
393 DOC concentrations than observed in the violin plots of both the discontinuous and sporadic
394 (Figure 2a). This change in DOC concentration's along the latitudinal gradient of the permafrost
395 zonation was also seen in the latitudinal gradient associated with ecoregion, where Arctic Tundra
396 and Sub-Arctic Tundra are found at higher latitudes than both boreal ecoregions (chi-square =
397 78, df = 3, *p* < 0.001; Figure 2b). The highest DOC concentrations were found in the continental
398 boreal (n = 389; 56 ± 56 mg L⁻¹) and Sub-Arctic Boreal (n = 442; 58 ± 97 mg L⁻¹) ecoregions,
399 and lowest in the Arctic Tundra (n = 1,209; 25 ± 75 mg L⁻¹) and Sub-Arctic Tundra (n = 493; 43
400 ± 61 mg L⁻¹) ecoregions. Inspection of the distribution of DOC concentrations across the
401 ecoregions highlights that the Arctic Tundra ecoregion had the highest density of samples at the
402 lowest DOC concentration (Figure 2b).

403 These latitudinal differences are also reflected in the observed differences (chi-square =
404 20, df = 3, *p* < 0.001) in DOC concentrations found within different soil classes. The highest
405 DOC concentrations are found within organic rich Histosol (n = 37; 61 ± 39 mg L⁻¹) and Histel
406 soils (n = 935; 53 ± 72 mg L⁻¹; Figure 2c), with the distribution of the data from these soils types
407 having a higher density at greater DOC concentrations (Figure 2c). Histel and Histosol soils are
408 the main type of permafrost soil found within the sporadic and discontinuous permafrost zone

409 and both boreal ecoregions (Hugelius et al., 2014). Mineral rich Orthels (n = 741; 38 ± 91 mg L⁻¹)
 410 ¹) and Turbels (n = 820; 31 ± 62 mg L⁻¹), mineral permafrost soils that have experienced
 411 cryoturbation, had the lowest DOC concentrations. The median DOC concentrations found
 412 within the top 3 m of these soil classes represent <1% of the soil organic carbon stock found in
 413 the top 3 m of each soil class (Hugelius et al., 2014). DOC concentrations also differed within
 414 the thermal horizon of these different soil classes (chi-square = 91, df = 3, $p < 0.001$; Figure 2d).
 415 The highest DOC concentrations were found in permafrost free sites (n = 202; 57 ± 22 mg L⁻¹),
 416 which were largely Histosol soils (19%) or Histel soils (74%) that have experienced thermokarst
 417 formation. In areas where permafrost was present, DOC concentrations were highest in the active
 418 layer (n = 1,400; 45 ± 74 mg L⁻¹) and the permafrost lens (n = 729; 30 ± 113 mg L⁻¹).



419

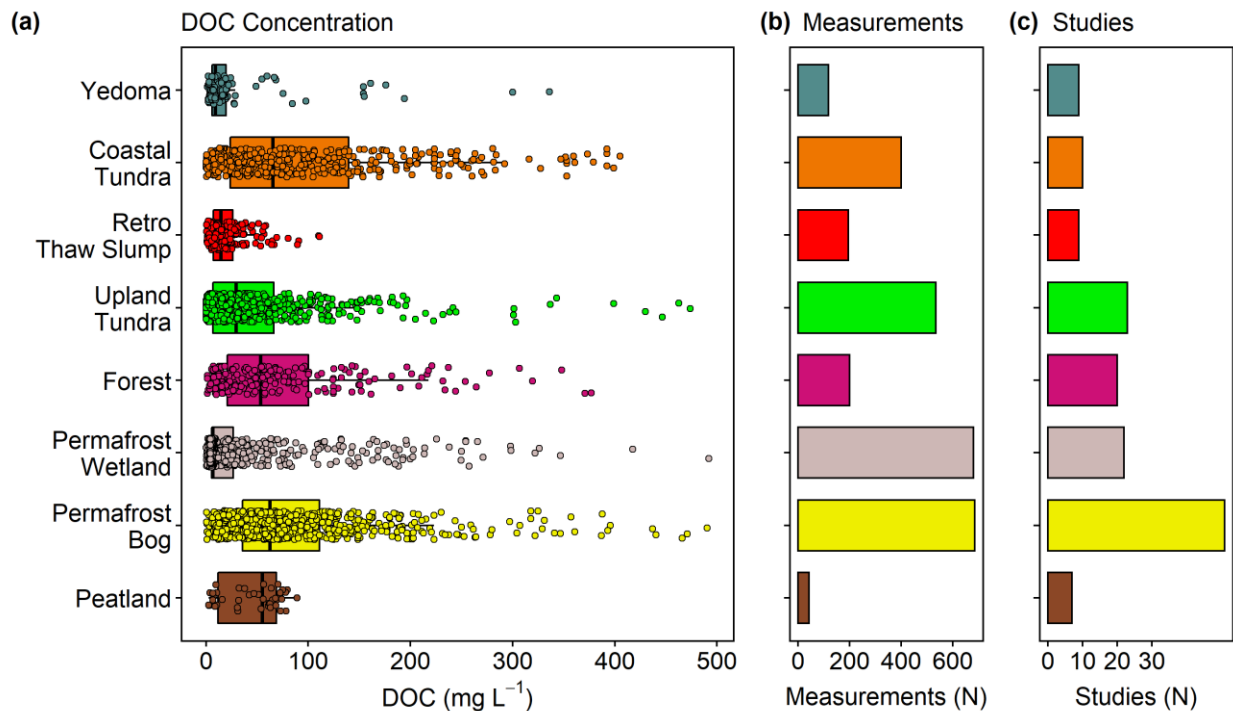
420 Figure 2. Violin plots of DOC concentrations (mg L⁻¹) found in the top 3 m across (a) permafrost
 421 zones, (b) ecoregions, (c) soil classes, and (d) thermal horizons. (a) Dark to light blue shading
 422 represents the permafrost zones Continuous, Discontinuous, and Sporadic, according to Brown
 423 et al., (1997). (b) Dark to light green shading represents the ecoregions Arctic Tundra, Sub-
 424 Arctic Tundra, Continental Boreal, and Sub-Arctic Boreal, according to Olson et al., (2001). (c)
 425 Dark to light yellow shading represents the soil classes Histosol, Histel, Orthel, and Turbel,

426 according to the USDA Soil Taxonomy (USDA, 1999). (d) Dark to light red shading represents
427 the thermal horizons Active Layer, Permafrost Lens, Thaw Stream, and Permafrost Free. Black
428 dots on each violin plot represents the median. Black vertical lines represent the interquartile
429 range with the upper and lower limits representing the 75th and 25th percentiles, respectively.
430 Either side of the black vertical line represents a kernel density estimation. This shape shows
431 the distribution of the data, with wider areas representing a higher probability that samples
432 within the database will have that DOC concentrations. The number of samples (n) found in
433 each sub-category is found above each corresponding violin plot.

434

435 *3.3 Trends in DOC concentrations across ecosystems*

436 Similar to other categorical variables (i.e. permafrost zone, ecoregion, soil class, and
437 thermal horizon data), DOC concentrations within each of the eight ecosystem types were found
438 to be non-normally distributed, with median values skewed toward the lower end of the 0 – 500
439 mg L⁻¹ range of concentrations (Figure S1). Permafrost bogs, upland tundra, and permafrost
440 wetlands were the most represented in the database with regards to DOC concentrations (Table
441 S1). The majority of permafrost bog measurements came from studies with field sites within
442 Canada (Figure 1; Table S1), as was the case for upland tundra and retrogressive thaw slump
443 DOC concentration data. The majority of permafrost wetland sample locations were found in
444 Russia, whereas the majority of the 414 coastal tundra sampling locations were in the USA. The
445 least represented ecosystem classes included the peatland ecosystem class, which is not strictly a
446 permafrost ecosystem as the other are, and the Yedoma ecosystem class (145 DOC
447 concentrations from 9 studies, Table S1). DOC concentrations differed significantly across the
448 eight ecosystem types (chi-square = 700, df = 7, $p < 0.001$; Figure 3). The highest DOC
449 concentrations were found in coastal tundra (66 ± 116 mg L⁻¹) and permafrost bogs (63 ± 75 mg
450 L⁻¹) ecosystems. The lowest DOC concentrations were found in permafrost wetlands (7 ± 20 mg
451 L⁻¹) and Yedoma ecosystems (9 ± 18 mg L⁻¹), both of which had only slightly lower median
452 DOC concentrations than retrogressive thaw slumps (15 ± 21 mg L⁻¹).



454

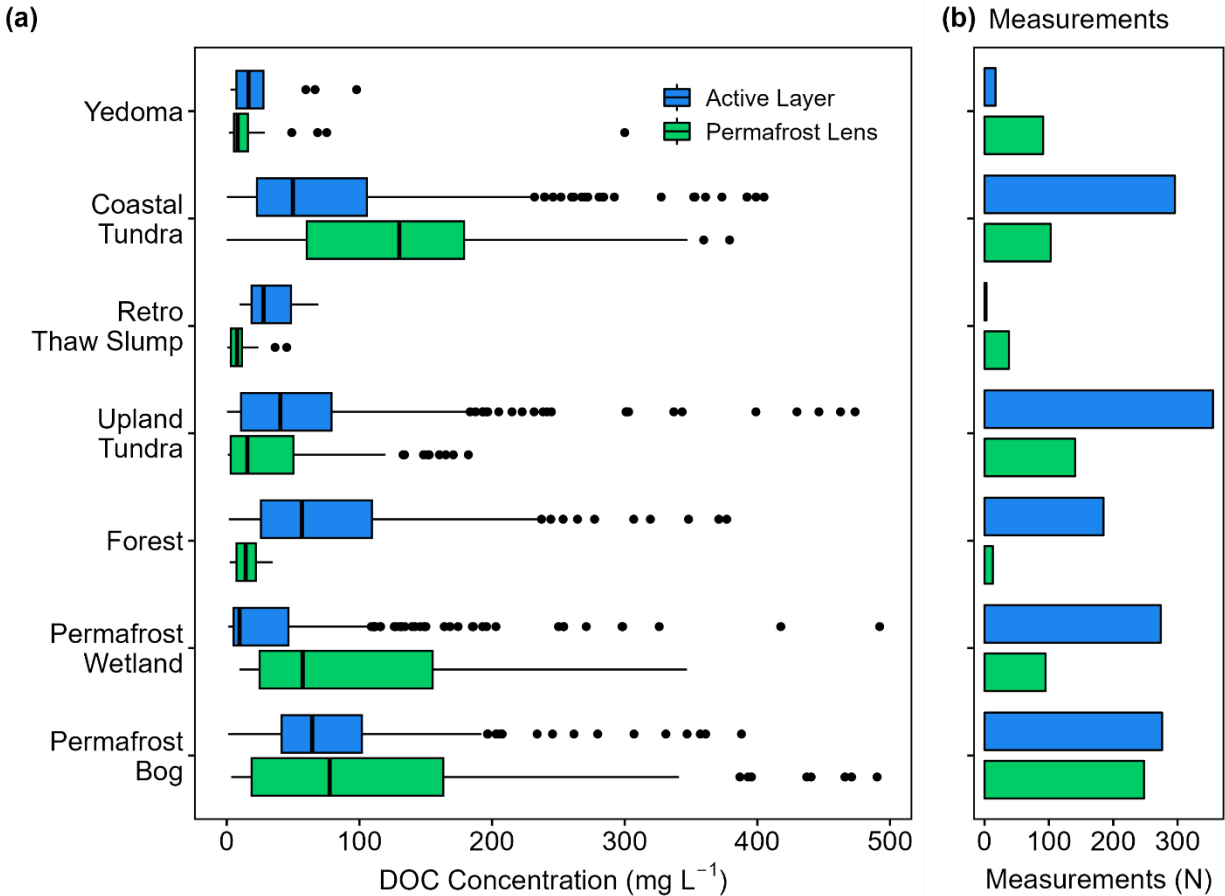
455 Figure 3. Boxplot and jitter plot of (a) DOC concentrations (mg L^{-1}), (b) the number of DOC
 456 measurements, and (c) number of studies including DOC measurements were taken from the
 457 top 3 m for each ecosystem type. Retro Thaw Slump = Retrogressive Thaw Slump. Boxes
 458 represents the interquartile range (25 – 75%), with median shown as black horizontal line.
 459 Whiskers extend to 1.5 times the interquartile range (distance between first and third quartile) in
 460 each direction. Jitter points represent the concentration of each individual DOC measurement,
 461 with random variation applied to each points location vertically in the plot, to avoid overplotting.
 462 Yedoma = dark teal. Coastal Tundra = orange. Retro Thaw Slump = red. Upland Tundra =
 463 green. Forest = purple. Permafrost Wetland = light pink. Permafrost bog = yellow. Peatland =
 464 brown.

465

466 When grouping all DOC concentrations by ecosystem types and differentiating between
 467 the active layer and permafrost lens thermal horizons, we found that DOC concentrations
 468 differed between the active layer and permafrost lens for all ecosystems (ANCOVA: $F_{(1, 1277)} =$
 469 $49.8, p < 0.001$), except for permafrost bogs (chi-square = 0.37, $df = 1, p = 0.5$) and Yedoma
 470 (chi-square = 3.5, $df = 1, p = 0.06$) ecosystems (Figure 4). Within the permafrost lens thermal
 471 horizon, the highest DOC concentrations were found in coastal tundra ($n = 103; 130 \pm 119 \text{ mg L}^{-1}$)
 472 and permafrost bogs ($n = 248; 78 \pm 144 \text{ mg L}^{-1}$) sites, and lowest found in Yedoma sites ($n =$
 473 $91; 8 \pm 10 \text{ mg L}^{-1}$). The highest active layer DOC concentrations were in permafrost bogs ($n =$

474 276; $64 \pm 61 \text{ mg L}^{-1}$) and forest ($n = 185$; $57 \pm 84 \text{ mg L}^{-1}$) sites, and lowest found in permafrost
 475 wetland sites ($n = 274$; $10 \pm 42 \text{ mg L}^{-1}$).

476



477

478 Figure 4 . Boxplot of (a) DOC concentrations (mg L^{-1}) and (b) the number of DOC
 479 measurements in the Active Layer and Permafrost Lens thermal horizons of each ecosystem
 480 type. Only DOC concentrations from ecosystems with these thermal horizons present is used,
 481 thus no permafrost-free sites are included. Retro Thaw Slump = Retrogressive Thaw Slump.
 482 Boxes represents the interquartile range (25 – 75%), with median shown as black horizontal
 483 line. Whiskers extend to 1.5 times the interquartile range (distance between first and third
 484 quartile) in each direction. Blue boxplots represent DOC concentrations in the active layer.
 485 Green boxplots represent DOC concentrations in the permafrost lens.

486

487 3.4 Effect of extraction and analysis methods on DOC concentrations

488 We found that DOC concentrations differed between filter sizes (ANOVA: $F_{(4, 2339)} =$
 489 $22.9, p < 0.001$) across. The highest DOC median concentrations reported were filtered using 0.45

490 μm ($53 \pm 78 \text{ mg L}^{-1}$) and $0.22 \mu\text{m}$ ($42 \pm 54 \text{ mg L}^{-1}$) and lowest using $0.7 \mu\text{m}$ ($17 \pm 78 \text{ mg L}^{-1}$).
491 The majority of DOC concentrations were determined using 0.45 , 0.7 , and $0.22 \mu\text{m}$ filter sizes.
492 The trends observed in in DOC concentrations across study regions and ecosystems were also
493 found when exploring these trends for the three main filter sizes used (Table S2, S3). Using 0.45
494 and $0.7 \mu\text{m}$ filter sizes, which represents 79% of all reported DOC concentrations, we find that
495 DOC concentrations are generally higher in the discontinuous and sporadic permafrost zone, the
496 two boreal ecoregions, Histel soils, and the active layer thermal horizons (Table S2). Similarly,
497 the highest DOC concentrations using these two most common filter sizes were highest in
498 permafrost bog and coastal tundra ecosystems (Table S3). Given these similarities when
499 considering and not considering filter size, and the large variation in DOC concentrations within
500 each filter size, we consider the effect of filter size on the trends observed in DOC concentrations
501 across study regions and ecosystems reported above (Figure 2, 3) to be minor.

502 DOC concentrations were found to be significantly different between samples subject to
503 the six broader groups of extraction method used (ANOVA: $F_{(5, 2518)} = 30.8$, $p < 0.001$), and
504 between water based and soil (solid) based extraction methods (ANOVA: $F_{(1, 2524)} = 182.1$, $p <$
505 0.001). The trends observed in in DOC concentrations across study regions (Figure 2) and
506 ecosystems (Figure 3) were also found when exploring study region and ecosystem trends for the
507 three main DOC extraction methods used (Table S4, S5). We found that 93% of DOC
508 concentrations were determined using the suction (42%), leach (37%), and grab (14%) extraction
509 methods. Using these three most common approaches the highest DOC concentrations across
510 study regions (Table S4) and ecosystems (Table S5) were found in the discontinuous and
511 sporadic permafrost zone, the two boreal ecoregions, Histel soils, the active layer thermal
512 horizons, and in permafrost bog and coastal tundra ecosystems.

513 The different methods of measuring DOC concentrations also produced significantly
514 different DOC concentrations (ANOVA: $F_{(3, 2515)} = 36.2$, $p < 0.001$). The three most common
515 accounted for 99% of all DOC concentrations and were combustion, persulphate, and
516 photometric. Of these three combustion was the most common and used for 89% of DOC
517 measurements. The persulphate and photometric methods were not used in all study regions
518 (Table S6) and ecosystems (Table S7), thus comparison of all three methods is not complete.
519 Trends in DOC measured using the combustion and persulphate method (Table S6, S7) were

520 similar to those found across study regions (Figure 2) and ecosystems (Figure 3). This is
521 unsurprising given that both of these methods account for 98% of all DOC concentrations.

522 We consider the effect of filter size, extraction method, and method of DOC
523 measurement to be minor in determining trends in DOC concentrations across study regions and
524 ecosystems. We find that trends in DOC concentrations across study regions and ecosystems are
525 similar when you both consider and do not consider the methods used to determine those
526 concentrations. Also, the variability observed in DOC concentrations for each study region and
527 ecosystem remains high even when considering filter size, extraction method, and measurement
528 method. Thus, each method or approach similarly impacts DOC concentrations from each study
529 region and ecosystem, and cannot explain the DOC concentration variability observed within
530 each. However, these different approaches did have an impact on DOC concentrations. In this
531 study we did not focus on systematically testing the effect of filter sizes, extraction methods, or
532 DOC measurement methods. Our goal was to assess the concentration and mobilization of DOC
533 in terrestrial permafrost ecosystems across circumpolar regions and ecosystems. The assessment
534 of methods is outside the scope of our study. Rather, we compare DOC concentrations collected
535 from samples using a variety of these methods and suggest that future studies use this
536 information to decide on methods to be consistent with compiled measurements, thus far.

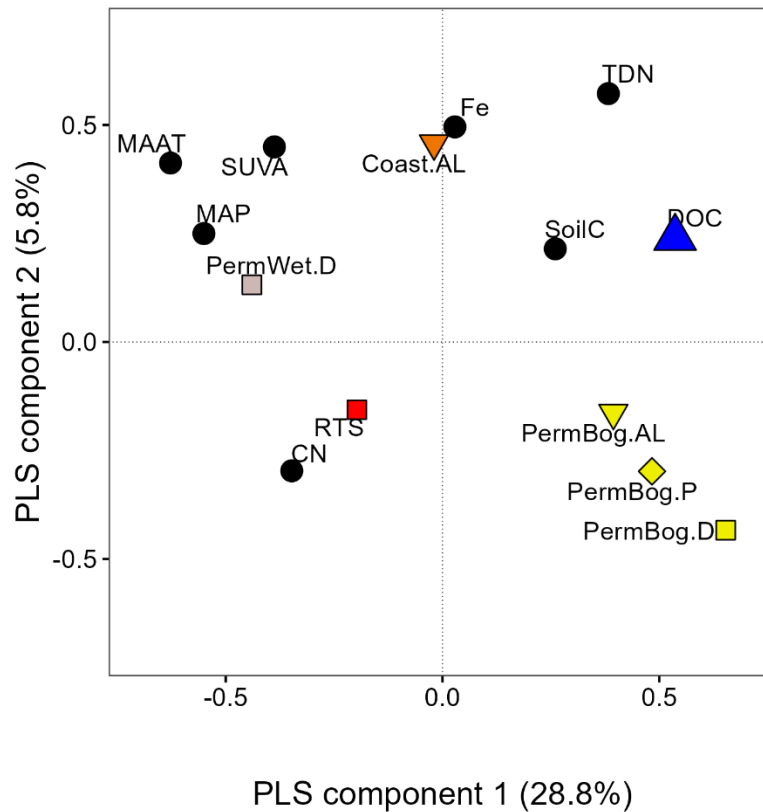
537 *3.5 Drivers of DOC concentrations*

538 No continuous variables recorded in the dataset were available for all DOC concentration
539 database entries, with no sites containing data for all continuous variables. This limited our
540 ability to explore relationships between continuous environmental and ecological data and DOC
541 concentrations across the permafrost region. To address drivers of DOC concentrations across
542 the circumpolar permafrost region we used partial least squares regression (PLS) as it is tolerant
543 to missing values. Multiple PLS regressions were run using various combinations of continuous
544 and categorical data with similar model performance throughout. We chose the PLS to determine
545 the drivers of DOC concentrations using environmental continuous variables and ecosystem type
546 as this contained the lowest background correlation. The most parsimonious PLS regression
547 extracted 9 significant components, captured 79% variation of the predictor variables, and
548 explained 37% of the variance in DOC concentrations in the dataset. The majority of the

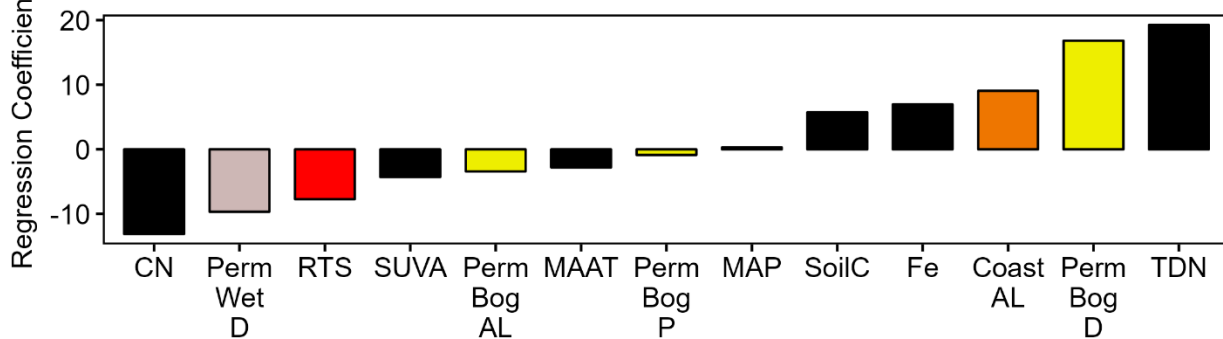
549 variance in DOC (35%) is explained along the first two axes of the model. The model was robust
550 and not overfitted as model predictability was moderate ($Q^2 = 0.35$) and background correlation
551 was low (0.006).

552 The PLS plot (Figure 5a) shows the correlation between DOC concentrations and
553 selected environmental and ecological variables for the first two axes of the model. The two
554 variables with the greatest positive and negative relationship with DOC concentrations were total
555 dissolved nitrogen content (mg L^{-1}) and C:N ratios, respectively (Figure 5b). The positive
556 relationship of DOC with total dissolved nitrogen and soil carbon content (SoilC), and negative
557 relationship with the specific UV absorbance at 254 nm (SUVA), may be a result of ecosystem
558 properties. The strong negative relationship with C:N ratios indicates that DOC concentrations
559 decrease with increased decomposition. Other than higher soil carbon content (SoilC) in
560 permafrost bogs, there was no clear or obvious observable trends in SoilC, TDN, C:N ratios, and
561 SUVA across ecosystem types (Figure S3). The PLS demonstrates that ecosystem type strongly
562 affects DOC concentrations, with DOC positively related with the highest ecosystems where the
563 highest DOC concentrations are observed, permafrost bogs and coastal tundra, and negatively
564 related to the lower DOC ecosystems, permafrost wetland and retrogressive thaw slumps (Figure
565 5). This negative relationship may be due to the higher latitudes these ecosystems are generally
566 found at, which is supported by the negative relationship with DOC and the climate indicators
567 mean annual temperature (MAAT) and mean annual precipitation (MAP). Additionally, it may
568 be due to the high number of thermokarst affected sites found within these ecosystem classes,
569 particularly retrogressive thaw slumps. There is a clear negative relationship between DOC
570 concentrations and disturbed permafrost wetlands, retrogressive thaw slumps, and permafrost
571 bogs.

(a)



(b)



573

574 Figure 5. Partial least squares regression (PLS) (a) loadings plot explaining 37% of the
 575 variability observed in DOC concentrations. (b) Bar plot of PLS regression coefficients showing
 576 the relative importance of each variable in predicting DOC concentrations. Regression
 577 coefficients on y-axis are normalized so their absolute sum is 100, with positive and negative
 578 values indicating the direction of the relationship. In the loadings plot squares depict ecosystem
 579 classes and the blue triangle represents DOC concentrations. Black circles in the (a) loadings
 580 plot and black bars in the (b) bar plot represent continuous environmental data that had at least
 581 20% coverage of DOC data. Continuous data variables are represented by the colour black. CN =
 582 carbon:nitrogen ratio. SUVA = the specific UV absorbance at 254 nm ($L\ mg\ C^{-1}\ m^{-1}$). MAP =

583 mean annual precipitation (mm). MAAT = mean annual temperature. SoilC = carbon content of
584 soil (g C kg⁻¹). TDN = total dissolved nitrogen (mg L⁻¹). Fe = dissolved iron (mg L⁻¹). PermWet.D
585 = disturbed permafrost wetland ecosystem class and is light pink (as in Figure 3) to represent
586 this ecosystem class. RTS = retrogressive thaw slump ecosystem class and is red (as in Figure
587 3) to represent this ecosystem class. Coast.AL = active layer of coastal tundra ecosystem class
588 and is orange. PermBog.AL = active layer of permafrost bog ecosystem class and is yellow.
589 PermBog.P = permafrost lens of permafrost bog ecosystem class and is yellow. PermBog.D =
590 disturbed permafrost bog ecosystem class and is yellow.

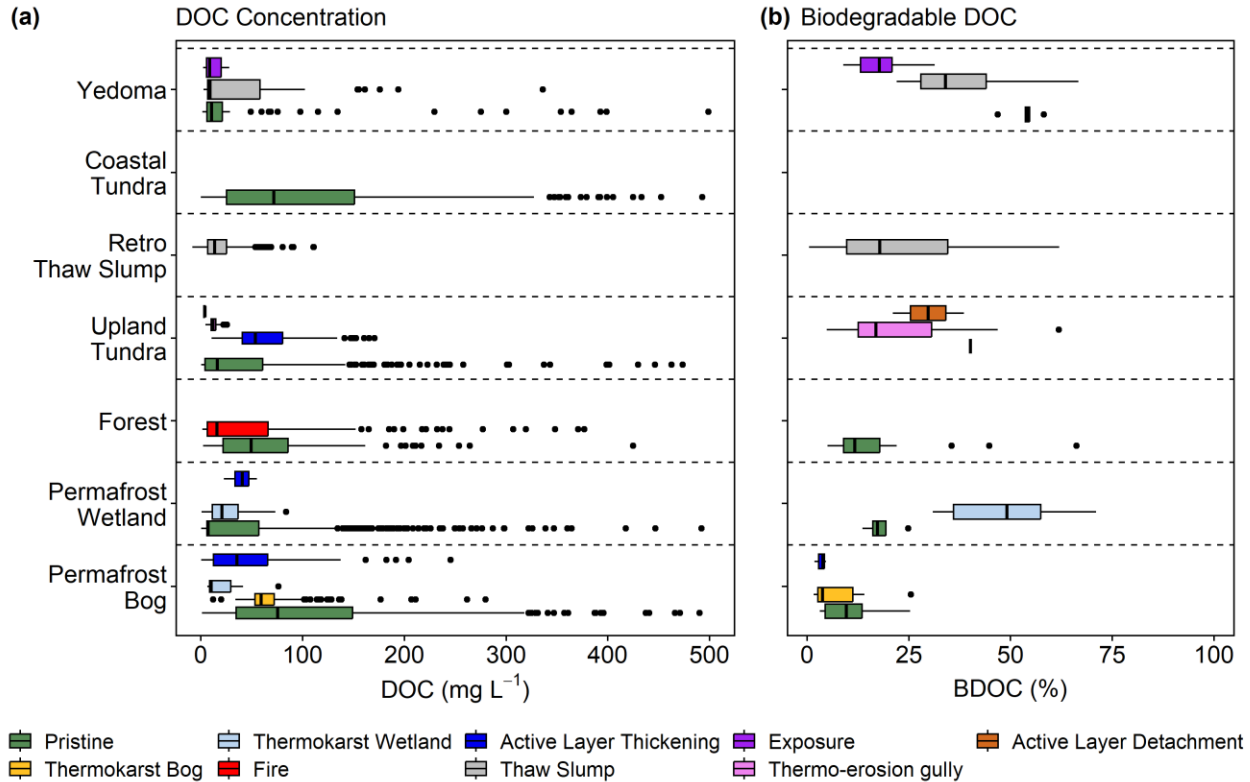
591 *3.6 Response and mobilization of DOC and BDOC to thermokarst formation*

592 The highest DOC concentrations were found in pristine permafrost bog (n = 442; 75 ±
593 112 mg L⁻¹) and coastal tundra ecosystems (n = 427; 72 ± 126 mg L⁻¹; Figure 6a). No
594 thermokarst affected coastal tundra ecosystems were recorded within the dataset. Whereas, in
595 permafrost bogs DOC concentrations were found to differ across different thermokarst
596 disturbances (ANOVA: $F_{(3, 720)} = 23.04, p < 0.001$), with the lowest found in thermokarst
597 wetlands (n = 16; 10 ± 21 mg L⁻¹). DOC concentrations were also found to differ between
598 thermokarst affected and pristine sites in upland tundra ecosystems (ANOVA: $F_{(3, 539)} = 5.91, p$
599 < 0.001). The highest DOC concentrations in upland tundra ecosystems were found in sites that
600 had experienced active layer thickening (n = 142; 53 ± 39 mg L⁻¹), whereas the lowest were
601 found in sites that had experienced active layer detachment (n = 6; 4 ± 2 mg L⁻¹). Pristine sites
602 had the highest DOC concentrations in both Yedoma (n = 114; 11 ± 15 mg L⁻¹) and forest (n =
603 189; 49 ± 64 mg L⁻¹) ecosystems. However, in permafrost wetland ecosystems pristine sites had
604 the lowest DOC concentrations (n = 766; 7 ± 51 mg L⁻¹) with sites that were affected by both
605 thermokarst wetland formation (n = 17; 21 ± 26 mg L⁻¹) and active layer thickening (n = 12; 41 ±
606 13 mg L⁻¹) having higher DOC concentrations.

607 Our database contained limited data regarding BDOC (n = 146), thus BDOC results
608 across ecosystems should be interpreted with caution. Due to limited data we have combined
609 BDOC over all incubation lengths when assessing BDOC between pristine and thermokarst sites
610 (Figure 6). BDOC was found to differ between thermokarst disturbances within ecosystem types
611 in only Yedoma (ANOVA: $F_{(2, 27)} = 23.09, p < 0.001$) and permafrost wetland (ANOVA: $F_{(1, 10)}$
612 $= 15.87, p < 0.001$) ecosystems. The highest BDOC was found in both of these ecosystem types
613 also, with 54% (n = 5) in pristine Yedoma sites and 49% (n = 8) in thermokarst wetland affected
614 permafrost wetland sites (Figure 6b), with the latter exhibiting the highest BDOC across all

615 permafrost affected sites followed by thaw slumps (18%, $n = 11$) in Yedoma ecosystems and
616 active layer thickening (40%, $n = 1$) in upland tundra sites. The lowest median BDOC of 4%
617 were seen in thermokarst bogs ($n = 5$) and active layer thickening ($n = 3$) affected sites, with
618 pristine sites experiencing BDOC of 9% ($n = 15$). However, not all ecosystem types in the
619 database had BDOC data for both pristine and disturbance sites. For example, only pristine sites
620 data was available for forests, whereas there was no pristine site data available for upland tundra
621 sites. No BDOC data was available for coastal tundra sites.

622 All ecosystem types that had BDOC data, reported BDOC observed following 40 – 90
623 incubation days, and this also corresponded to the highest BDOC values for each ecosystem type
624 (Figure S4). When comparing the greatest BDOC observed within this incubation length
625 window, we found that values varied across ecosystem type (ANOVA: $F_{(5, 131)} = 14.6$, $p <$
626 0.001). The highest loss rates were observed in Yedoma and permafrost wetland ecosystems,
627 whereas the lowest we observed in organic rich forest and permafrost bog ecosystems (Figure
628 S4). Forest (ANOVA: $F_{(1, 16)} = 2.31$, $p = 0.15$) and permafrost bog (ANOVA: $F_{(3, 24)} = 2.49$, $p =$
629 0.09) BDOC did not differ over incubation length, whereas Yedoma (ANOVA: $F_{(4, 25)} = 24.92$, p
630 < 0.001) and permafrost wetland (ANOVA: $F_{(1, 10)} = 15.87$, $p < 0.01$) did differ over time, with
631 their max occurring during this 40 – 90-day incubation length. This suggests that when incubated
632 for the same number of days, we would expect greater BDOC in Yedoma and permafrost
633 wetland ecosystems. Note, for this analysis BDOC values from all thermokarst and non-
634 thermokarst affected sites within an ecosystem type were included. Given the limited BDOC data
635 available we have compared BDOC across ecosystems in two ways. The first is using data from
636 all measurement days to assess BDOC across pristine and disturbed ecosystems (Figure 6b). The
637 second is assessing max BDOC within each ecosystem type, which includes pristine and
638 disturbed sites (Figure S4). Using both approaches we find that the highest BDOC is observed in
639 high-latitude Yedoma and permafrost wetland sites.



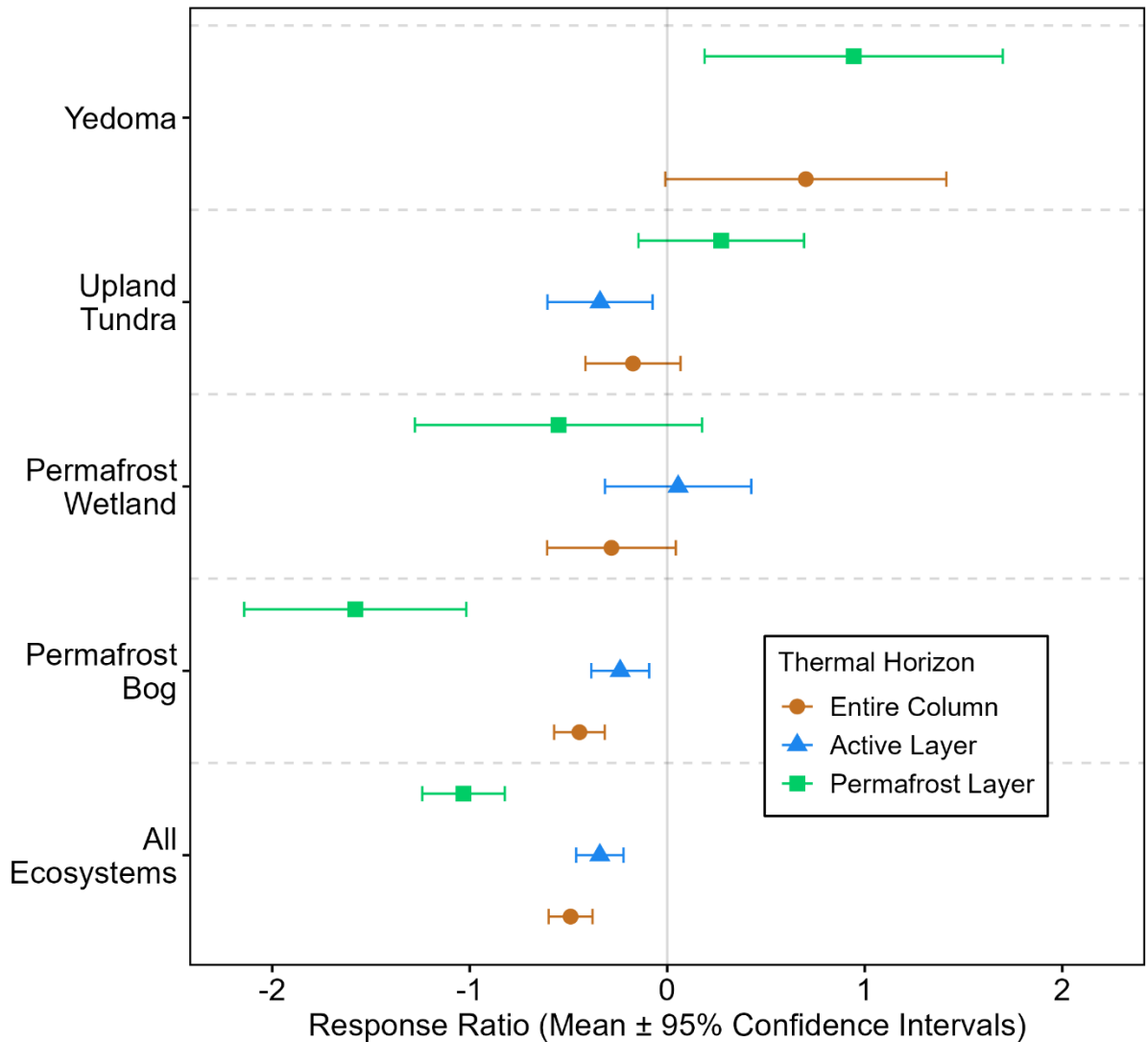
640

641 Figure 6. DOC concentrations (mg L^{-1}) and biodegradable DOC (BDOC; %) from the top 3 m
 642 following disturbance including data from both field based and incubation studies. (a) DOC
 643 concentrations from each ecosystem type following disturbance where data was available. (b)
 644 Biodegradable DOC (BDOC) from each ecosystem type following disturbance where data was
 645 available. BDOC loss was determined following 3 – 304 days of incubation. Data from different
 646 incubation lengths was combined due to low sample size. Retro Thaw Slump = Retrogressive
 647 Thaw Slump. Boxes represents the interquartile range (25 – 75%), with median shown as black
 648 horizontal line. Whiskers extend to 1.5 times the interquartile range (distance between first and
 649 third quartile) in each direction, with outlier data plotted individually as black dots. Note colours
 650 associated with boxplots in this figure are only relevant for this figure.

651 Response ratios comparing the change in DOC concentrations between pristine and
 652 thermokarst affected sites were calculated from our dataset from 108 studies using Eq. 1 (Figure
 653 7). Only 17 studies provided data for both pristine and thermokarst affected ecosystems, with 87
 654 papers providing DOC concentrations from pristine and 34 from thermokarst affected sites.
 655 When considering all ecosystems together we found that response ratios were negative,
 656 suggesting that DOC concentrations were higher in thermokarst affected sites compared to
 657 pristine sites (Figure 7). These negative response ratios were most evident in permafrost bogs,
 658 where they found throughout the entire column and individual thermal horizons. The greatest

659 increase in DOC concentrations following thermokarst was seen when comparing DOC
660 concentrations in the permafrost lens of permafrost bogs, and to a lesser extent permafrost
661 wetlands (Figure 7). Only in Yedoma ecosystems did we see positive response ratios throughout
662 the entire profile, suggesting a decrease in DOC concentrations following thermokarst formation
663 in Yedoma sites. This was also seen for DOC concentrations within the permafrost lens of
664 upland tundra sites, which include DOC concentrations from retrogressive thaw slumps and
665 thermo-erosion gullies in their thermokarst affected sites. The large confidence intervals for
666 some response ratios suggests high variability in the response of DOC concentrations to
667 thermokarst formation.

668



669

670 Figure 7. Response ratios of DOC concentrations from the top 3 m following thermokarst
 671 formation (calculated using Eq. 1). Response ratio means allow for relative comparison of
 672 changes in DOC following thermokarst formation between different ecosystem types. Negative
 673 values indicate lower DOC concentrations found in pristine ecosystems, whereas positive value
 674 indicates a decrease in DOC concentrations following thermokarst. Studies reporting DOC
 675 concentrations from Exposures, Retrogressive Thaw Slumps, and Thermo-Erosion Gullies from
 676 sites within the continuous permafrost zone were combined into the Upland Tundra ecosystem
 677 category. This did not include DOC concentrations from studies within the Yedoma permafrost
 678 domain (Strauss et al., 2021). Blue line represent DOC concentrations in the active layer, as per
 679 Figure 4. Green lines represent DOC concentrations in the permafrost lens, as per Figure 4.

680 Brown lines represent DOC concentrations from the entire column (i.e., both active layer and
681 permafrost lens).

682 **4. Discussion**

683 In this systematic review, we evaluated patterns of DOC concentrations in the top 3 m of
684 soil in terrestrial ecosystems across the northern circumpolar permafrost region based on results
685 from 111 studies and 2,845 DOC measurements. We focused on comparing concentrations of
686 DOC in soils across various geographical regions, ecological conditions, and disturbance types.
687 Our synthesis shows that median DOC concentrations across ecosystems range from 9 – 61 mg
688 L⁻¹, which represents similar albeit slightly higher DOC concentrations when compared to the
689 median DOC concentrations found in top soils of other land cover groups below 50°N (25 mg L⁻¹
690 ¹; Langeveld et al., 2020), globally distributed lakes (6 mg L⁻¹; Sobek et al., 2007), and lakes
691 across the permafrost region (11 mg L⁻¹; Stolpmann et al., 2021). In general, we show that
692 organic soils have higher DOC concentrations than mineral soils, and that DOC concentrations
693 are positively related to total dissolved nitrogen concentrations and negatively to C:N ratios,
694 which corroborate previous findings of factors correlating with DOC concentrations (Aitkenhead
695 & McDowell, 2000; Lajtha et al., 2005). Overall, we found that properties associated with
696 ecosystem type are the main constraint on DOC concentrations. Furthermore, disturbance
697 through permafrost thaw has little impact on measured DOC concentrations, however this may
698 be due to the loss of biologically reactive DOC or the loss of an initially larger pulse of DOC
699 having been previously mobilised prior to the timing of sampling.

700 *4.1 Environmental factors influencing DOC*

701 Our database confirmed our first hypothesis that the highest DOC concentrations would be
702 found in organic rich soils. Previous synthesis efforts estimating global distributions of terrestrial
703 DOC concentrations have presented similar findings (Guo et al., 2020; Langeveld et al., 2020).
704 Both of these previous studies also show that some of the highest terrestrial DOC concentrations
705 are found within the northern circumpolar permafrost region, highlighting that these high DOC
706 concentrations found in organic rich permafrost soils are of global significance. Concentrations
707 of DOC in the top 3 m of soils closely mirrored stocks of SOC across the circumpolar permafrost
708 region (Hugelius et al., 2014). Organic rich Histosol and Histel soils contain the greatest SOC

709 per km², followed by Turbels and Orthels (Hugelius et al., 2014). The leaching of organic C from
710 soils act as a major source of DOC (Kalbitz et al., 2000; Marschner & Bredow, 2002), thus it is
711 not surprising that we find the highest DOC concentrations in the soil types with the greatest
712 quantities of SOC (Figure 2a). While the highest DOC concentrations are found within organic
713 rich soils, the amount of C found as DOC represent a small amount of the total SOC pool. Using
714 the current best estimates of Histel SOC stocks (Hugelius et al., 2020), the DOC pool represents
715 <1% of the total C stock in permafrost-affected peatlands as has been shown for both permafrost
716 and global soils (Guo et al., 2020; Prokushkin et al., 2008).

717 *4.2 Variation in DOC across ecosystems*

718 The accumulation of high DOC concentrations we show in permafrost bogs and permafrost
719 wetlands (Figure 3), is a result of the prevalence of cold and anoxic conditions throughout the
720 Holocene (Blodau, 2002). This leads to a reduction in microbial decomposition, and the
721 accumulation of both a large SOC (Hugelius et al., 2020) and DOC pool. Our results suggest that
722 the pristine permafrost bog and permafrost wetland DOC pool is relatively stable following
723 permafrost thaw (Figure 6, 7a). The lower DOC pool found in the active layer of permafrost
724 wetland (Figure 4a) may represent a potentially labile DOC pool (Figure 7a), but this is likely due
725 to fresh, plant derived inputs rather than the exposure and mineralization of previously frozen
726 organic matter (Figure 7a). Peatland vegetation, in particular *Sphagnum* mosses, produces litter
727 that has anti-microbial properties and is decay resistant (Hamard et al., 2019; Limpens, Bohlin,
728 & Nilsson, 2017), limiting the amount of SOC that is degraded and assimilated into the DOC
729 pool (Tfaily et al., 2013). This is further enhanced by the build-up of decomposition end products
730 and the thermodynamic constraint on decay observed in anoxic soils (Beer et al., 2008).
731 Permafrost has been continuously present in peatlands across the northern circumpolar
732 permafrost region for the past 6,000 years, with the greatest rates of permafrost formation
733 occurring within the past 3,000 years (Treat & Jones, 2018). Thus, a large proportion of the
734 organic matter found peatlands and wetlands in this region were present prior to permafrost
735 aggradation (i.e., permafrost formation), which indicates that permafrost formed epigenetically in
736 these areas. Permafrost aggradation impacts soil biogeochemical properties, leading to
737 potentially less decomposed organic matter with higher C/N ratios than non-permafrost
738 equivalent soils, particularly in permafrost wetlands (Treat et al., 2016). This can lead to the

739 build-up of high DOC concentrations that are vulnerable to potential mobilization following
740 thermokarst. Decomposition in epigenetic permafrost bogs following thermokarst has been
741 shown to be relatively slow (Heffernan et al., 2020; Manies et al., 2021), which further supports
742 our finding (Figure 6) that the large DOC pool found in these systems is relatively stable
743 following permafrost thaw.

744 Coastal tundra ecosystems had similarly high DOC concentrations to those found in
745 permafrost bogs (Figure 3a). Coastal tundra ecosystems represented the highest concentrations of
746 DOC in mineral permafrost soils, with the highest concentrations found in the permafrost lens
747 (Figure 4a). This is contrary to findings that deeper coastal permafrost consists of low organic
748 matter Pleistocene marine sediments (Bristol et al., 2021) and the proximity of the active layer to
749 vegetation inputs, although this productivity and inputs are vulnerable to projected climatic
750 warming and regional “browning” and “greening” (Lara et al., 2018). Recent work has shown
751 that DOC in the active layer within the coastal permafrost is more biodegradable than OC in the
752 permafrost lens (Speetjens et al., 2022) and a substantial proportion of organic carbon derived
753 from thawing coastal permafrost is vulnerable to mineralization upon thawing, particularly when
754 exposed to sea water (Tanski et al., 2021). Export of terrestrial coastal permafrost DOC directly
755 into the Arctic Ocean can significantly influence marine biogeochemical cycles and food webs
756 within the Arctic ocean (Bruhn et al., 2021). Arctic coasts are eroding at rates of up to 25 m yr⁻¹
757 (Fritz, Vonk, & Lantuit, 2017) and exporting large quantities of terrestrial organic matter export
758 directly to the ocean that is rapidly mineralized (Tanski et al., 2019). Enhanced DOC export from
759 these coastal tundra ecosystems may disrupt aquatic food webs through altering nutrient and
760 light supply, as has been shown for Swedish coastal systems (Peacock et al., 2022). These
761 coastal tundra sites represent a large DOC pool that is highly vulnerable to enhanced
762 mobilization and deserve further attention.

763 We found that DOC concentrations increased along a clear latitudinal gradient, from north to
764 south, in the remaining ecosystems characterised by mineral soils with an upper organic layer,
765 i.e., forests, upland tundra, and Yedoma. In forest ecosystems, the upper organic layer, and the
766 impact of soil temperature, moisture, and pH on SOC found there, strongly influences the
767 production, concentration, and composition of DOC (Neff & Hooper, 2002; Wickland et al.,
768 2007). Furthermore, the sorption of DOC to charcoal (Guggenberger et al., 2008), and high

769 lignin and phenolic input from vegetation (O'Donnell et al., 2016) produce a difficult to degrade
770 DOC pool, leading to the accumulation of the large DOC pool in the active layer (Figure 4a) this
771 ecosystem type. This trend with depth has also been observed in the vertical distribution of DOC
772 across global soils, with 50% of the DOC pool found in the top 0 – 30 cm (Guo et al., 2020).
773 While not included in the most parsimonious PLS model (Figure 5), Yedoma and upland tundra
774 ecosystems were found to negatively correlate with DOC concentrations (Figure S5). The
775 greatest proportions of OC and nutrients used for DOC production in these ecosystems are found
776 in shallow organic layers (Semenchuk et al., 2015; Wild et al., 2013). Beneath the upper organic
777 horizons in these mineral soils processes such as sorption of DOC to minerals and the formation
778 of Fe-DOC or Al-DOC complexes may remove DOC from the dissolved pool (Kawahigashi et
779 al., 2006) and mechanically protect it from mobilization (Gentsch et al., 2015). The majority of
780 vegetation and its leachates found in the permafrost region produce relatively stable DOC
781 consisting of lignin-derived compounds, highly aromatic polyphenolic compounds, and low
782 molecular weight organic acids (Chen et al., 2018; Drake et al., 2015; Ewing et al., 2015; Selvam
783 et al., 2017). While differences in the stability of different DOC source end-members have been
784 shown (MacDonald et al., 2021), differences in redox conditions are likely a major driver in
785 differences in the accumulation and mineralization of DOC across permafrost ecosystem types
786 (Mohammed et al., 2022).

787 *4.3 Vulnerability of DOC to enhanced mobilization following thermokarst*

788 We define DOC mobilization as DOC lost from an ecosystem either via export or
789 degradation. Our second hypothesis that permafrost thaw would lead to enhanced mobilization of
790 DOC cannot be fully supported by the findings from this database. Using our chosen systematic
791 approach and focusing on data from terrestrial ecosystems, our database was limited to 3 studies
792 which represented <1% of the DOC concentration data. Several previous studies have detailed
793 the export of DOC in Arctic inland waters, see Table 2 in Ma et al., (2019). These studies were
794 excluded using our systematic approach (Table 1 and 2) as they do not directly measure DOC
795 export from a terrestrial ecosystem, rather they determine the quantity of terrestrial derived DOC
796 found in inland waters. This is a key distinction, as by not quantifying the export rates for
797 terrestrial ecosystems the net ecosystem carbon balance and vulnerability to enhanced export
798 may not be assessed.. We acknowledge the limitation in our approach regarding the inclusion of

799 DOC export data. Thus, this database cannot be used to determine how permafrost thaw will
800 influence DOC export from terrestrial ecosystems within the northern circumpolar permafrost
801 region. However, we identify this lack of export data from terrestrial permafrost ecosystems as a
802 key knowledge gap in our current understanding of the permafrost carbon pool. Currently, Arctic
803 rivers are estimated to export 25 – 36 Tg DOC year⁻¹ (Amon et al., 2012; Holmes et al., 2012),
804 with this being dominated by modern carbon sources (Estop-Aragonés et al., 2020), most likely
805 derived from the top 1 m of terrestrial ecosystems. Using current best estimates of the areal
806 extent and soil organic carbon stores in the top 1 m of Histosols, Histels, Orthels and Turbels
807 (Hugelius et al., 2014), and if we assume that the DOC pool represents ~1% of the SOC pool, we
808 estimate that <1% of the current DOC pool found in the top 1 m of Histosols, Histels, Orthels
809 and Turbels is exported annually to Arctic rivers. Quantifying the proportion of these DOC pools
810 annually lost, and particularly the proportions lost in headwater streams while being exported to
811 Arctic rivers, is vital to assess the importance of the mobilization of the terrestrial permafrost
812 DOC pool.

813 Our calculated response ratios (Figure 7) for all ecosystems, indicating the difference in DOC
814 concentrations between pristine and permafrost thaw affected sites, partly supports our second
815 hypothesis that disturbance would lead to increased export and biodegradability of DOC. The
816 increase in DOC following thaw observed in permafrost bogs is likely due to increased inputs
817 due to increased runoff and shifts in vegetation following permafrost thaw (Burd, Estop-
818 Aragonés, Tank, & Olefeldt, 2020), enhanced release of DOC (Loiko et al., 2017), a relatively
819 stable soil organic carbon pool at depth due to several millennia of microbial processing (Manies
820 et al., 2021), the prevalence of anoxic conditions, and the potential hydrological isolation of
821 thermokarst bogs (Quinton, Hayashi, & Pietroniro, 2003). While not included in our analysis,
822 DOC found near the surface of the permafrost lens in forest ecosystems has been shown to be
823 more biodegradable than DOC found in the active layer (Wickland et al., 2018), and may
824 represent a decrease in DOC following thermokarst not captured here. Our findings of limited
825 mobilization of permafrost bog DOC upon thawing are supported by the findings that the ¹⁴C
826 signature of DOC in Arctic rivers is dominated by modern sources (Estop-Aragonés et al., 2020).
827 However, individual studies have determined that thawing may release a large pool of permafrost
828 peatland DOC into aquatic networks (Lim et al., 2021). We do see a reduction in DOC

829 concentrations in thermokarst affected sites at the higher latitude Yedoma, upland tundra, and
830 permafrost wetland ecosystems. This reduction in DOC concentrations in these ecosystems may
831 be due to the greater biodegradability and lability of the DOC found there (Figure 6b),
832 supporting our third hypothesis that the most biodegradable DOC would be found in higher
833 latitude ecosystems. Permafrost DOC in higher latitude ecosystems, particularly Yedoma
834 ecosystems, is characterised by syngenetic permafrost aggradation which have not undergone
835 centuries to millennia of soil formation and microbial processes, have been shown contain a
836 greater proportion of low oxygen, aliphatic compounds and labile substrates (Ewing et al.,
837 2015b; MacDonald et al., 2021). This leads to a greater biolability and rapid mineralization of
838 DOC (Vonk et al., 2015), potentially causing the reduction in DOC concentrations observed
839 following thaw. If this hypothesis is to be found true across all high latitude ecosystems with
840 further data, it further highlights the vulnerability of the large DOC pool found in coastal tundra
841 ecosystems.

842 In this study, we focus on the dissolved fraction of the OC pool, however the particulate
843 fraction should also be considered when discussing the mobilization of terrestrial OC in
844 permafrost landscapes. In boreal freshwater networks, particulate organic carbon (POC)
845 represents a small but highly labile fraction of terrestrially derived OC exported to the fluvial
846 network (Attermeyer et al., 2018). The degradation of permafrost derived POC is much slower
847 than that of POC in the boreal freshwater network and POC derived from younger sources along
848 the riverbank (Shakil, Tank, Kokelj, Vonk, & Zolkos, 2020). The DOC pool in Arctic
849 freshwaters is dominated by modern terrestrial sources (Estop-Aragonés et al., 2020), whereas
850 the POC pool has been shown to be dominated by older sources in both permafrost peatland
851 dominated areas (Wild et al., 2019), following the formation of retrogressive thaw slumps
852 (Keskitalo et al., 2021), and in thermokarst affected periglacial streams (Bröder et al., 2022).
853 This older POC has been shown to accumulate following export due to low lability and
854 degradation and mineral association, which suggests that upon thermokarst formation, previously
855 frozen OC exported in the particulate phase is not readily consumed by microbes and that
856 permafrost derived DOC is the more labile fraction of exported terrestrial OC.

857 *4.4 Future considerations for study design*

858 Determining the fate of mobilized terrestrial DOC in both permafrost thaw affected, and
859 pristine sites should be prioritized in future studies to constrain current estimates of the
860 permafrost C climate feedback. There are large spatial gaps in the database, particularly in areas
861 with large stock of permafrost C such as the Hudson Bay Lowlands and Mackenzie River Basin,
862 both in Canada and two of the three largest deposits of permafrost peatland C in the circumpolar
863 permafrost region (Olefeldt et al., 2021). Similarly, coastal tundra sites, which along with
864 permafrost bog represent the ecosystems with the highest DOC concentrations, were sampled
865 only along the northern shoreline of Alaska and the Yukon (USA and Canada, respectively;
866 Table S1). From our analysis of this database, we determine that DOC mobilization is poorly
867 understood for terrestrial permafrost ecosystems. To address this, the two main needs of future
868 studies are 1) more direct estimates of DOC fluxes and export from terrestrial ecosystems into
869 aquatic ecosystems, and 2) more DOC degradation (BDOC) and mineralization studies. Our
870 results suggest that the high concentrations of DOC in permafrost bogs remains relatively stable
871 upon thermokarst formation, although individual studies do indicate that thawing peat may
872 provide a reactive source of DOC (Panneer Selvam et al., 2017). The database did not include
873 any studies that reported on the mineralization of DOC from coastal tundra sites, thus we are
874 unable to comment on the stability of the high DOC concentrations found in this ecosystem type.
875 Further sampling and assessing the mineralization of DOC is required to characterize the
876 potential pool of vulnerable DOC in areas with high DOC concentrations. Overall, our database
877 and systematic approach only included 5 studies (Olefeldt & Roulet, 2012, 2014; Olefeldt et al.,
878 2012; Prokushkin et al., 2006; Prokushkin et al., 2005) that explicitly reported rates of DOC
879 discharge, export, or fluxes from terrestrial ecosystems into the fluvial network. Given the
880 importance of terrestrial DOC as a source for CO₂ production within the aquatic network
881 (Weyhenmeyer et al., 2012), and the findings that previously frozen DOC is being exported to
882 the freshwater network (Estop-Aragones et al., 2020), improved estimates of the quantity of
883 terrestrial DOC being exported is essential to determine the potential aquatic greenhouse gas
884 fluxes derived from the mineralization of terrigenous organic matter. To improve current
885 estimates of the permafrost C feedback further studies are needed to determine how much DOC
886 is laterally exported from terrestrial ecosystems, and the mineralization potential of this DOC
887 along the terrestrial-freshwater-aquatic continuum.

888 Lastly, we suggest that future studies should consider a standardization of methods and
889 approached used to determine DOC concentrations for better comparison across studies. In
890 constructing this database we identified three different filter sizes, eleven different extraction
891 procedures, and four different measurement methods. The most common filter size used was
892 0.45 μm and this has previously been described as the cut off to separate DOC from colloid
893 materials (Thurman 1985; Bolan et al., 1999). In extracting DOC concentrations from soils the
894 mostly commonly used approach (70% of all soil samples) was via soil leaching with no
895 chemical treatment of the soils, although some added filtered water to promote leaching. From
896 the seven approaches identified to extract water samples from terrestrial sites in determining
897 DOC, 48% of samples were collected using a variety of suction devices and 46% done via grab
898 samples. Of the four DOC measurements methods the most common approach was by
899 combustion, with 90% of all DOC concentrations measured using this approach. As such, in
900 order to continue measuring DOC concentrations in terrestrial permafrost ecosystems using the
901 most consistent approach we suggest using 0.45 μm filters, extracting pore water via some type
902 of sucking device or soils via leaching, and using a combustion based method to determine DOC
903 concentrations

904 **Data availability**

905 All data will be made freely and publicly available on an online repository prior to publication

906 **Author contributions**

907 LH, DK, and LT designed and planned the systematic review approach; LH built the database.
908 LH and DK analyzed the data; LH wrote the manuscript draft; DK and LT edited and reviewed
909 the manuscript.

910 **Competing interests**

911 The authors declare that they have no conflict of interest.

912 **Acknowledgements**

913 We thank Konstantinos Vaziourakis, Mona Abbasi, Elizabeth Jakobsson, Marloes Groeneveld,
914 Sarah Shakil, and Jeffrey Hawkes for helpful discussions throughout the development and
915 writing of this manuscript.

916 **Financial support**

917 This work was supported by the Knut and Alice Wallenberg Foundation. DK was funded from
918 the Swedish National Science Foundation (VR 2020-03249).

919 **References (in text)**

920 Abbott, B. W., Larouche, J. R., Jones, J. J. B., Bowden, W. B., & Balser, A. W. (2014). From
921 Thawing and Collapsing Permafrost. *Journal of Geophysical Research: Biogeosciences*,
922 119, 2049–2063. <https://doi.org/10.1002/2014JG002678>. Received

923 Aitkenhead, J. A., & McDowell, W. H. (2000). Soil C:N ratio as a predictor of annual riverine
924 DOC flux at local and global scales. *Global Biogeochemical Cycles*, 14(1).
925 <https://doi.org/10.1029/1999GB900083>

926 Amon, R. M. W., Rinehart, A. J., Duan, S., Louchouart, P., Prokushkin, A., Guggenberger, G.,
927 ... Zhulidov, A. V. (2012). Dissolved organic matter sources in large Arctic rivers.
928 *Geochimica et Cosmochimica Acta*, 94, 217–237.
929 <https://doi.org/https://doi.org/10.1016/j.gca.2012.07.015>

930 Andersen, C.M. and Bro, R. (2010), Variable selection in regression—a tutorial. *J.*
931 *Chemometrics*, 24: 728-737. <https://doi.org/10.1002/cem.1360>

932 Andresen, C. G., Lawrence, D. M., Wilson, C. J., McGuire, A. D., Koven, C., Schaefer, K.,
933 Jafarov, E., Peng, S., Chen, X., Gouttevin, I., Burke, E., Chadburn, S., Ji, D., Chen, G.,
934 Hayes, D., and Zhang, W.: Soil moisture and hydrology projections of the permafrost region
935 – a model intercomparison, *The Cryosphere*, 14, 445–459, [https://doi.org/10.5194/tc-14-](https://doi.org/10.5194/tc-14-445-2020)
936 445-2020, 2020.

937 Arksey, H., & O'Malley, L. (2005). Scoping studies: Towards a methodological framework.
938 *International Journal of Social Research Methodology: Theory and Practice*, 8(1).
939 <https://doi.org/10.1080/1364557032000119616>

940 Attermeyer, K., Catalán, N., Einarsdottir, K., Freixa, A., Groeneveld, M., Hawkes, J. A., ...
941 Tranvik, L. J. (2018). Organic Carbon Processing During Transport Through Boreal Inland
942 Waters: Particles as Important Sites. *Journal of Geophysical Research: Biogeosciences*,
943 123(8). <https://doi.org/10.1029/2018JG004500>

944 Beckebanze, L., Runkle, B. R. K., Walz, J., Wille, C., Holl, D., Helbig, M., ... Kutzbach, L.

- 945 (2022). Lateral carbon export has low impact on the net ecosystem carbon balance of a
 946 polygonal tundra catchment. *BIOGEOSCIENCES*, 19(16), 3863–3876.
 947 <https://doi.org/10.5194/bg-19-3863-2022>
- 948 Beer, J., Lee, K., Whiticar, M., & Blodau, C. (2008). Geochemical controls on anaerobic organic
 949 matter decomposition in a northern peatland. *Limnology and Oceanography*, 53(4), 1393–
 950 1407. <https://doi.org/10.4319/lo.2008.53.4.1393>
- 951 Biester, H., Knorr, K. H., Schellekens, J., Basler, A., & Hermanns, Y. M. (2014). Comparison of
 952 different methods to determine the degree of peat decomposition in peat bogs.
 953 *Biogeosciences*. <https://doi.org/10.5194/bg-11-2691-2014>
- 954 Blodau, C. (2002). Carbon cycling in peatlands — A review of processes and controls.
 955 *Environmental Reviews*, 10(2), 111–134. <https://doi.org/10.1139/a02-004>
- 956 Bolan, N.S., Baskaran, S., Thiagarajan, S. (1999). Methods of Measurement of Dissolved
 957 Organic Carbon of Plant Origin in Soils, Manures, Sludges and Stream Water. In: Linskens,
 958 H.F., Jackson, J.F. (eds) Analysis of Plant Waste Materials. Modern Methods of Plant
 959 Analysis, vol 20. Springer, Berlin, Heidelberg. https://doi.org/10.1007/978-3-662-03887-1_1
 960
- 961 Bristol, E. M., Connolly, C. T., Lorenson, T. D., Richmond, B. M., Ilgen, A. G., Choens, R. C.,
 962 ... McClelland, J. W. (2021). Geochemistry of Coastal Permafrost and Erosion-Driven
 963 Organic Matter Fluxes to the Beaufort Sea Near Drew Point, Alaska. *Frontiers in Earth
 964 Science*, 8. <https://doi.org/10.3389/feart.2020.598933>
- 965 Bröder, L., Hirst, C., Opfergelt, S., Thomas, M., Vonk, J. E., Haghypour, N., ... Fouché, J.
 966 (2022). Contrasting Export of Particulate Organic Carbon From Greenlandic Glacial and
 967 Nonglacial Streams. *Geophysical Research Letters*, 49(21).
 968 <https://doi.org/10.1029/2022GL101210>
- 969 Brown, J., Ferrians Jr., O. J., Heginbottom, J. A., & Melnikov, E. S. (1997). Circum-Arctic map
 970 of permafrost and ground ice conditions. *USGS Numbered Series*, 1.
 971 <https://doi.org/10.1016/j.jallcom.2010.03.054>
- 972 Bruhn, A. D., Stedmon, C. A., Comte, J., Matsuoka, A., Speetjens, N. J., Tanski, G., ... Sjöstedt,
 973 J. (2021). Terrestrial Dissolved Organic Matter Mobilized From Eroding Permafrost
 974 Controls Microbial Community Composition and Growth in Arctic Coastal Zones.
 975 *Frontiers in Earth Science*, 9. <https://doi.org/10.3389/feart.2021.640580>
- 976 Burd, K., Estop-Aragónés, C., Tank, S. E., & Olefeldt, D. (2020). Lability of dissolved organic
 977 carbon from boreal peatlands: interactions between permafrost thaw, wildfire, and season.
 978 *Canadian Journal of Soil Science*, 13(February), 1–13. <https://doi.org/10.1139/cjss-2019-0154>
 979
- 980 Camill, P. (2005). Permafrost thaw accelerates in boreal peatlands during late-20th century

- 981 climate warming. *Climatic Change*, 68(1–2), 135–152. [https://doi.org/10.1007/s10584-005-](https://doi.org/10.1007/s10584-005-4785-y)
982 4785-y
- 983 Chanton, J. P., Glaser, P. H., Chasar, L. S., Burdige, D. J., Hines, M. E., Siegel, D. I., ... Cooper,
984 W. T. (2008). Radiocarbon evidence for the importance of surface vegetation on
985 fermentation and methanogenesis in contrasting types of boreal peatlands. *Global*
986 *Biogeochemical Cycles*, 22(4), 1–11. <https://doi.org/10.1029/2008GB003274>
- 987 Chen, H., Yang, Z., Chu, R. K., Tolic, N., Liang, L., Graham, D. E., ... Gu, B. (2018). Molecular
988 Insights into Arctic Soil Organic Matter Degradation under Warming. *ENVIRONMENTAL*
989 *SCIENCE & TECHNOLOGY*, 52(8), 4555–4564. <https://doi.org/10.1021/acs.est.7b05469>
- 990 Chong, I. G., & Jun, C. H. (2005). Performance of some variable selection methods when
991 multicollinearity is present. *Chemometrics and Intelligent Laboratory Systems*, 78(1).
992 <https://doi.org/10.1016/j.chemolab.2004.12.011>
- 993 Connon, R. F., Quinton, W. L., Craig, J. R., & Hayashi, M. (2014). Changing hydrologic
994 connectivity due to permafrost thaw in the lower Liard River valley, NWT, Canada.
995 *Hydrological Processes*, 28(14). <https://doi.org/10.1002/hyp.10206>
- 996 Dean, J. F., Meisel, O. H., Rosco, M. M., Marchesini, L. B., Garnett, M. H., Lenderink, H., ...
997 Dolman, A. J. (2020). East Siberian Arctic inland waters emit mostly contemporary carbon.
998 *NATURE COMMUNICATIONS*, 11(1). <https://doi.org/10.1038/s41467-020-15511-6>
- 999 Drake, T. W., Wickland, K. P., Spencer, R. G. M., McKnight, D. M., & Striegl, R. G. (2015).
1000 Ancient low-molecular-weight organic acids in permafrost fuel rapid carbon dioxide
1001 production upon thaw. *PROCEEDINGS OF THE NATIONAL ACADEMY OF SCIENCES*
1002 *OF THE UNITED STATES OF AMERICA*, 112(45), 13946–13951.
1003 <https://doi.org/10.1073/pnas.1511705112>
- 1004 Ernakovich, J. G., Lynch, L. M., Brewer, P. E., Calderon, F. J., & Wallenstein, M. D. (2017).
1005 Redox and temperature-sensitive changes in microbial communities and soil chemistry
1006 dictate greenhouse gas loss from thawed permafrost. *BIOGEOCHEMISTRY*, 134(1–2),
1007 183–200. <https://doi.org/10.1007/s10533-017-0354-5>
- 1008 Estop-Aragones, C., Olefeldt, D., Abbott, B. W., Chanton, J. P., Czimczik, C. I., Dean, J. F., ...
1009 Anthony, K. W. (2020). Assessing the Potential for Mobilization of Old Soil Carbon After
1010 Permafrost Thaw: A Synthesis of C-14 Measurements From the Northern Permafrost
1011 Region. *GLOBAL BIOGEOCHEMICAL CYCLES*, 34(9).
1012 <https://doi.org/10.1029/2020GB006672>
- 1013 Estop-Aragónés, Cristian, Czimczik, C. I., Heffernan, L., Gibson, C., Walker, J. C., Xu, X., &
1014 Olefeldt, D. (2018). Respiration of aged soil carbon during fall in permafrost peatlands
1015 enhanced by active layer deepening following wildfire but limited following thermokarst.
1016 *Environmental Research Letters*, 13(8). <https://doi.org/10.1088/1748-9326/aad5f0>
- 1017 Ewing, S. A., Paces, J. B., O'Donnell, J. A., Jorgenson, M. T., Kanevskiy, M. Z., Aiken, G. R.,

- 1018 ... Striegl, R. (2015a). Uranium isotopes and dissolved organic carbon in loess permafrost:
 1019 Modeling the age of ancient ice. *GEOCHIMICA ET COSMOCHIMICA ACTA*, 152, 143–
 1020 165. <https://doi.org/10.1016/j.gca.2014.11.008>
- 1021 Ewing, S. A., Paces, J. B., O'Donnell, J. A., Jorgenson, M. T., Kanevskiy, M. Z., Aiken, G. R.,
 1022 ... Striegl, R. (2015b). Uranium isotopes and dissolved organic carbon in loess permafrost:
 1023 Modeling the age of ancient ice. *Geochimica et Cosmochimica Acta*, 152, 143–165.
 1024 <https://doi.org/10.1016/j.gca.2014.11.008>
- 1025 Fouché, J., Christiansen, C. T., Lafrenière, M. J., Grogan, P., & Lamoureux, S. F. (2020).
 1026 Canadian permafrost stores large pools of ammonium and optically distinct
 1027 dissolved organic matter. *Nature Communications*, 11(1), 4500.
 1028 <https://doi.org/10.1038/s41467-020-18331-w>
- 1029 Fritz, M., Vonk, J. E., & Lantuit, H. (2017). Collapsing Arctic coastlines. *Nature Climate*
 1030 *Change*. <https://doi.org/10.1038/nclimate3188>
- 1031 Gentsch, N., Mikutta, R., Shibistova, O., Wild, B., Schnecker, J., Richter, A., ... Guggenberger,
 1032 G. (2015). Properties and bioavailability of particulate and mineral-associated organic
 1033 matter in Arctic permafrost soils, Lower Kolyma Region, Russia. *European Journal of Soil*
 1034 *Science*, 66(4). <https://doi.org/10.1111/ejss.12269>
- 1035 Guggenberger, G., & Zech, W. (1993). Dissolved organic carbon control in acid forest soils of
 1036 the Fichtelgebirge (Germany) as revealed by distribution patterns and structural
 1037 composition analyses. *Geoderma*, 59(1–4). [https://doi.org/10.1016/0016-7061\(93\)90065-S](https://doi.org/10.1016/0016-7061(93)90065-S)
- 1038 Guggenberger, Georg, Rodionov, A., Shibistova, O., Grabe, M., Kasansky, O. A., Fuchs, H., ...
 1039 Flessa, H. (2008). Storage and mobility of black carbon in permafrost soils of the forest
 1040 tundra ecotone in Northern Siberia. *Global Change Biology*, 14(6), 1367–1381.
 1041 <https://doi.org/10.1111/j.1365-2486.2008.01568.x>
- 1042 Guo, Z., Wang, Y., Wan, Z., Zuo, Y., He, L., Li, D., ... Xu, X. (2020). Soil dissolved organic
 1043 carbon in terrestrial ecosystems: Global budget, spatial distribution and controls. *Global*
 1044 *Ecology and Biogeography*, 29(12). <https://doi.org/10.1111/geb.13186>
- 1045 Hamard, S., Robroek, B. J. M., Allard, P. M., Signarbieux, C., Zhou, S., Saesong, T., ... Jassey,
 1046 V. E. J. (2019). Effects of Sphagnum Leachate on Competitive Sphagnum Microbiome
 1047 Depend on Species and Time. *Frontiers in Microbiology*, 10.
 1048 <https://doi.org/10.3389/fmicb.2019.02042>
- 1049 Hansen, A. M., Kraus, T. E. C., Pellerin, B. A., Fleck, J. A., Downing, B. D., & Bergamaschi, B.
 1050 A. (2016). Optical properties of dissolved organic matter (DOM): Effects of biological and
 1051 photolytic degradation. *Limnology and Oceanography*, 61(3), 1015–
 1052 1032. <https://doi.org/10.1002/lno.10270>
- 1053 Heffernan, L., Cavaco, M. A., Bhatia, M. P., Estop-Aragónés, C., Knorr, K.-H., & Olefeldt, D.

- 1054 (2022). High peatland methane emissions following permafrost thaw: enhanced acetoclastic
 1055 methanogenesis during early successional stages. *Biogeosciences*, 19(12).
 1056 <https://doi.org/10.5194/bg-19-3051-2022>
- 1057 Heffernan, L., Estop-Aragonés, C., Knorr, K.-H., Talbot, J., & Olefeldt, D. (2020). Long-term
 1058 impacts of permafrost thaw on carbon storage in peatlands: deep losses offset by surficial
 1059 accumulation. *Journal of Geophysical Research: Biogeosciences*, 2011(2865),
 1060 e2019JG005501. <https://doi.org/10.1029/2019JG005501>
- 1061 Heslop, J. K., Chandra, S., Sobczak, W. V, Davydov, S. P., Davydova, A. I., Spektor, V. V, &
 1062 Anthony, K. M. W. (2017). Variable respiration rates of incubated permafrost soil extracts
 1063 from the Kolyma River lowlands, north-east Siberia. *POLAR RESEARCH*, 36.
 1064 <https://doi.org/10.1080/17518369.2017.1305157>
- 1065 Holmes, R. M., McClelland, J. W., Peterson, B. J., Tank, S. E., Bulygina, E., Eglinton, T. I., ...
 1066 Zimov, S. A. (2012). Seasonal and Annual Fluxes of Nutrients and Organic Matter from
 1067 Large Rivers to the Arctic Ocean and Surrounding Seas. *ESTUARIES AND COASTS*, 35(2),
 1068 369–382. <https://doi.org/10.1007/s12237-011-9386-6>
- 1069 Hugelius, G., Strauss, J., Zubrzycki, S., Harden, J. W., Schuur, E. A. G., Ping, C. L., ... Kuhry,
 1070 P. (2014). Estimated stocks of circumpolar permafrost carbon with quantified uncertainty
 1071 ranges and identified data gaps. *Biogeosciences*, 11(23), 6573–6593.
 1072 <https://doi.org/10.5194/bg-11-6573-2014>
- 1073 Hugelius, Gustaf, Loisel, J., Chadburn, S., Jackson, R. B., Jones, M., MacDonald, G., ... Yu, Z.
 1074 (2020). Large stocks of peatland carbon and nitrogen are vulnerable to permafrost thaw.
 1075 *Proceedings of the National Academy of Sciences*, 117(34), 20438–20446.
 1076 <https://doi.org/10.1073/pnas.1916387117>
- 1077 Hultman, J., Waldrop, M. P., Mackelprang, R., David, M. M., McFarland, J., Blazewicz, S. J., ...
 1078 Jansson, J. K. (2015). Multi-omics of permafrost, active layer and thermokarst bog soil
 1079 microbiomes. *Nature*, 521(7551). <https://doi.org/10.1038/nature14238>
- 1080 Jorgenson, M. T., Shur, Y. L., & Pullman, E. R. (2006). Abrupt increase in permafrost
 1081 degradation in Arctic Alaska. *Geophysical Research Letters*, 33(2).
 1082 <https://doi.org/10.1029/2005GL024960>
- 1083 Kalbitz K, Sloinger S, Park JH, Michalzik B, Matzner E (2000) Controls on the dynamics of
 1084 dissolved organic matter in soils: a review. *Soil Science*, 165, 277–304.
- 1085 Kawahigashi, M., Kaiser, K., Rodionov, A., & Guggenberger, G. (2006). Sorption of dissolved
 1086 organic matter by mineral soils of the Siberian forest tundra. *GLOBAL CHANGE*
 1087 *BIOLOGY*, 12(10), 1868–1877. <https://doi.org/10.1111/j.1365-2486.2006.01203.x>
- 1088 Keskitalo, K. H., Bröder, L., Shakil, S., Zolkos, S., Tank, S. E., van Dongen, B. E., ... Vonk, J.
 1089 E. (2021). Downstream Evolution of Particulate Organic Matter Composition From

- 1090 Permafrost Thaw Slumps. *Frontiers in Earth Science*, 9.
1091 <https://doi.org/10.3389/feart.2021.642675>
- 1092 Kicklighter, D. W., Hayes, D. J., McClelland, J. W., Peterson, B. J., McGuire, A. D., & Melillo,
1093 J. M. (2013). Insights and issues with simulating terrestrial DOC loading of Arctic river
1094 networks. *ECOLOGICAL APPLICATIONS*, 23(8), 1817–1836. <https://doi.org/10.1890/11-1050.1>
1095
- 1096 Kokelj, S. V., & Jorgenson, M. T. (2013). Advances in thermokarst research. *Permafrost and*
1097 *Periglacial Processes*, 24(2), 108–119. <https://doi.org/10.1002/ppp.1779>
- 1098 Lajeunesse, M. J. (2011). On the meta-analysis of response ratios for studies with correlated and
1099 multi-group designs. *Ecology*, 92(11). <https://doi.org/10.1890/11-0423.1>
- 1100 Lajtha, K., Crow, S. E., Yano, Y., Kaushal, S. S., Sulzman, E., Sollins, P., & Spears, J. D. H.
1101 (2005). Detrital controls on soil solution N and dissolved organic matter in soils: A field
1102 experiment. *Biogeochemistry*, 76(2). <https://doi.org/10.1007/s10533-005-5071-9>
- 1103 Lamit, L. J., Romanowicz, K. J., Potvin, L. R., Lennon, J. T., Tringe, S. G., Chimner, R. A., ...
1104 Lilleskov, E. A. (2021). Peatland microbial community responses to plant functional group
1105 and drought are depth-dependent. *Molecular Ecology*, 30(20).
1106 <https://doi.org/10.1111/mec.16125>
- 1107 Langeveld, J., Bouwman, A. F., van Hoek, W. J., Vilmin, L., Beusen, A. H. W., Mogollón, J. M.,
1108 & Middelburg, J. J. (2020). Estimating dissolved carbon concentrations in global soils: a
1109 global database and model. *SN Applied Sciences*, 2(10), 1–21.
1110 <https://doi.org/10.1007/s42452-020-03290-0>
- 1111 Lantuit, H., Overduin, P. P., Couture, N., Wetterich, S., Aré, F., Atkinson, D., Brown, J.,
1112 Cherkashov, G., Drozdov, D., Forbes, D. L., & Graves-Gaylord, A. (2012). The Arctic
1113 coastal dynamics database: A new classification scheme and statistics on Arctic permafrost
1114 coastlines. *Estuaries and Coasts*, 35(2), 383–400. <https://doi.org/10.1007/s12237-010-9362-6>
1115
- 1116 Lara, M. J., Nitze, I., Grosse, G., Martin, P., & David McGuire, A. (2018). Reduced arctic tundra
1117 productivity linked with landform and climate change interactions. *Scientific Reports*, 8(1).
1118 <https://doi.org/10.1038/s41598-018-20692-8>
- 1119 Liljedahl, A. K., Boike, J., Daanen, R. P., Fedorov, A. N., Frost, G. V., Grosse, G., ... Zona, D.
1120 (2016). Pan-Arctic ice-wedge degradation in warming permafrost and its influence on
1121 tundra hydrology. *Nature Geoscience*, 9(4). <https://doi.org/10.1038/ngeo2674>
- 1122 Limpens, J., Bohlin, E., & Nilsson, M. B. (2017). Phylogenetic or environmental control on the
1123 elemental and organo-chemical composition of Sphagnum mosses? *Plant and Soil*.
1124 <https://doi.org/10.1007/s11104-017-3239-4>

- 1125 Loiko, S. V, Pokrovsky, O. S., Raudina, T. V, Lim, A., Kolesnichenko, L. G., Shirokova, L. S.,
 1126 ... Kirpotin, S. N. (2017). Abrupt permafrost collapse enhances organic carbon, CO₂,
 1127 nutrient and metal release into surface waters. *Chemical Geology*, 471, 153–165.
 1128 <https://doi.org/https://doi.org/10.1016/j.chemgeo.2017.10.002>
- 1129 Ma, Q., Jin, H., Yu, C., & Bense, V. F. (2019). Dissolved organic carbon in permafrost regions:
 1130 A review. *Science China Earth Sciences*. <https://doi.org/10.1007/s11430-018-9309-6>
- 1131 MacDonald, E. N., Tank, S. E., Kokelj, S. V., Froese, D. G., & Hutchins, R. H. S. (2021).
 1132 Permafrost-derived dissolved organic matter composition varies across permafrost end-
 1133 members in the western Canadian Arctic. *Environmental Research Letters*, 16(2).
 1134 <https://doi.org/10.1088/1748-9326/abd971>
- 1135 Manies, K. L., Jones, M. C., Waldrop, M. P., Leewis, M. C., Fuller, C., Cornman, R. S., &
 1136 Hoefke, K. (2021). Influence of Permafrost Type and Site History on Losses of Permafrost
 1137 Carbon After Thaw. *Journal of Geophysical Research: Biogeosciences*, 126(11).
 1138 <https://doi.org/10.1029/2021JG006396>
- 1139 Marschner B, Bredow A (2002) Temperature effects on release and ecologically relevant
 1140 properties of dissolved organic carbon in sterilised and biologically active soil samples. *Soil*
 1141 *Biology and Biochemistry*, 34, 459–466.
- 1142 McGuire, A. D., Lawrence, D. M., Koven, C., Klein, J. S., Burke, E., Chen, G., ... Zhuang, Q.
 1143 (2018). Dependence of the evolution of carbon dynamics in the northern permafrost region
 1144 on the trajectory of climate change. *Proceedings of the National Academy of Sciences of the*
 1145 *United States of America*, 115(15). <https://doi.org/10.1073/pnas.1719903115>
- 1146 Mehmood, T., Liland, K. H., Snipen, L., & Sæbø, S. (2012). A review of variable selection
 1147 methods in Partial Least Squares Regression. *Chemometrics and Intelligent Laboratory*
 1148 *Systems*. <https://doi.org/10.1016/j.chemolab.2012.07.010>
- 1149 Mevik, B. H., & Wehrens, R. (2007). The pls package: Principal component and partial least
 1150 squares regression in R. *Journal of Statistical Software*, 18(2).
 1151 <https://doi.org/10.18637/jss.v018.i02>
- 1152 Miner, K. R., Turetsky, M. R., Malina, E., Bartsch, A., Tamminen, J., McGuire, A. D., ... Miller,
 1153 C. E. (2022). Permafrost carbon emissions in a changing Arctic. *Nature Reviews Earth and*
 1154 *Environment*. <https://doi.org/10.1038/s43017-021-00230-3>
- 1155 Mohammed, A. A., Guimond, J. A., Bense, V. F., Jamieson, R. C., McKenzie, J. M., & Kurylyk,
 1156 B. L. (2022). Mobilization of subsurface carbon pools driven by permafrost thaw and
 1157 reactivation of groundwater flow: a virtual experiment. *Environmental Research Letters*,
 1158 17(12), 124036. <https://doi.org/10.1088/1748-9326/ACA701>
- 1159 Monteux, S., Weedon, J. T., Blume-Werry, G., Gavazov, K., Jassey, V. E. J., Johansson, M., ...
 1160 Dorrepaal, E. (2018). Long-term in situ permafrost thaw effects on bacterial communities

- 1161 and potential aerobic respiration. *ISME Journal*, 12(9), 2129–2141.
1162 <https://doi.org/10.1038/s41396-018-0176-z>
- 1163 Moore, T. R., & Dalva, M. (2001). Some controls on the release of dissolved organic carbon by
1164 plant tissues and soils. *Soil Science*, 166(1), 38–47. [https://doi.org/10.1097/00010694-](https://doi.org/10.1097/00010694-200101000-00007)
1165 [200101000-00007](https://doi.org/10.1097/00010694-200101000-00007)
- 1166 Neff, J. C., & Hooper, D. U. (2002). Vegetation and climate controls on potential CO₂, DOC and
1167 DON production in northern latitude soils. *Global Change Biology*, 8(9), 872–884.
1168 <https://doi.org/10.1046/j.1365-2486.2002.00517.x>
- 1169 O'Donnell, J. A., Aiken, G. R., Butler, K. D., Guillemette, F., Podgorski, D. C., & Spencer, R.
1170 G. M. (2016). DOM composition and transformation in boreal forest soils: The effects of
1171 temperature and organic-horizon decomposition state. *Journal of Geophysical Research:*
1172 *Biogeosciences*, 121(10), 2727–2744. <https://doi.org/10.1002/2016JG003431>.Received
- 1173 Olefeldt, D., Heffernan, L., Jones, M. C., Sannel, A. B. K., Treat, C. C., & Turetsky, M. R.
1174 (2021). Permafrost Thaw in Northern Peatlands: Rapid Changes in Ecosystem and
1175 Landscape Functions (pp. 27–67). https://doi.org/10.1007/978-3-030-71330-0_3
- 1176 Olefeldt, D., & Roulet, N. T. (2012). Effects of permafrost and hydrology on the composition
1177 and transport of dissolved organic carbon in a subarctic peatland complex. *Journal of*
1178 *Geophysical Research: Biogeosciences*, 117(1). <https://doi.org/10.1029/2011JG001819>
- 1179 Olefeldt, D., & Roulet, N. T. (2014). Permafrost conditions in peatlands regulate magnitude,
1180 timing, and chemical composition of catchment dissolved organic carbon export. *GLOBAL*
1181 *CHANGE BIOLOGY*, 20(10), 3122–3136. <https://doi.org/10.1111/gcb.12607>
- 1182 Olefeldt, D., Roulet, N. T., Bergeron, O., Crill, P., Bäckstrand, K., & Christensen, T. R. (2012).
1183 Net carbon accumulation of a high-latitude permafrost palsamire similar to permafrost-free
1184 peatlands. *Geophysical Research Letters*, 39(3). <https://doi.org/10.1029/2011GL050355>
- 1185 Olefeldt, D., Goswami, S., Grosse, G., Hayes, D., Hugelius, G., Kuhry, P., ... Turetsky, M. R.
1186 (2016). Circumpolar distribution and carbon storage of thermokarst landscapes. *Nature*
1187 *Communications*, 7, 13043. <https://doi.org/10.1038/ncomms13043>
- 1188 Olson, D. M., Dinerstein, E., Wikramanayake, E. D., Burgess, N. D., Powell, G. V. N.,
1189 Underwood, E. C., ... others. (2001). Terrestrial Ecoregions of the World: A New Map of
1190 Life on Earth: A new global map of terrestrial ecoregions provides an innovative tool for
1191 conserving biodiversity. *BioScience*, 51(11).
- 1192 Panneer Selvam, B., Lapierre, J.-F., Guillemette, F., Voigt, C., Lamprecht, R. E., Biasi, C., ...
1193 Berggren, M. (2017). Degradation potentials of dissolved organic carbon (DOC) from
1194 thawed permafrost peat. *SCIENTIFIC REPORTS*, 7, 45811.
1195 <https://doi.org/10.1038/srep45811>

- 1196 Parmentier, F.J.W., Christensen, T.R., Rysgaard, S. et al. A synthesis of the arctic terrestrial and
 1197 marine carbon cycles under pressure from a dwindling cryosphere. *Ambio* 46 (Suppl 1), 53–
 1198 69 (2017). <https://doi.org/10.1007/s13280-016-0872-8>
- 1199 Payandi-Rolland, D., Shirokova, L. S., Tesfa, M., Bénézech, P., Lim, A. G., Kuzmina, D., ...
 1200 Pokrovsky, O. S. (2020). Dissolved organic matter biodegradation along a hydrological
 1201 continuum in permafrost peatlands. *Science of The Total Environment*, 749, 141463.
 1202 <https://doi.org/10.1016/J.SCITOTENV.2020.141463>
- 1203 Peacock, M., Futter, M. N., Jutterström, S., Kothawala, D. N., Moldan, F., Stadmark, J., &
 1204 Evans, C. D. (2022). Three Decades of Changing Nutrient Stoichiometry from Source to
 1205 Sea on the Swedish West Coast. *Ecosystems*, 25(8). <https://doi.org/10.1007/s10021-022-00798-x>
- 1207 Pries, C. E. H., Schuur, E. A. G., & Crummer, K. G. (2012). Holocene Carbon Stocks and
 1208 Carbon Accumulation Rates Altered in Soils Undergoing Permafrost Thaw. *Ecosystems*,
 1209 15(1). <https://doi.org/10.1007/s10021-011-9500-4>
- 1210 Prokushkin, A. S., Gavrilenko, I. V., Abaimov, A. P., Prokushkin, S. G., & Samusenko, A. V.
 1211 (2006). Dissolved organic carbon in upland forested watersheds underlain by continuous
 1212 permafrost in Central Siberia. *Mitigation and Adaptation Strategies for Global Change*,
 1213 11(1), 223–240. <https://doi.org/10.1007/s11027-006-1022-6>
- 1214 Prokushkin, A S, Kajimoto, T., Prokushkin, S. G., McDowell, W. H., Abaimov, A. P., &
 1215 Matsuura, Y. (2005). Climatic factors influencing fluxes of dissolved organic carbon from
 1216 the forest floor in a continuous-permafrost Siberian watershed. *CANADIAN JOURNAL OF*
 1217 *FOREST RESEARCH*, 35(9), 2130–2140. <https://doi.org/10.1139/X05-150>
- 1218 Prokushkin, Anatoly S., Kawahigashi, M., & Tokareva, I. V. (2008). Global Warming and
 1219 Dissolved Organic Carbon Release from Permafrost Soils. In *Permafrost Soils* (pp. 237–
 1220 250). https://doi.org/10.1007/978-3-540-69371-0_16
- 1221 Quinton, W. L., Hayashi, M., & Chasmer, L. E. (2011). Permafrost-thaw-induced land-cover
 1222 change in the Canadian subarctic: Implications for water resources. *Hydrological Processes*,
 1223 25(1), 152–158. <https://doi.org/10.1002/hyp.7894>
- 1224 Quinton, W. L., Hayashi, M., & Pietroniro, A. (2003). Connectivity and storage functions of
 1225 channel fens and flat bogs in northern basins. *Hydrological Processes*.
 1226 <https://doi.org/10.1002/hyp.1369>
- 1227 Rantanen, M., Karpechko, A., Lipponen, A., Nordling, K., Hyvärinen, O., Ruosteenoja, K., ...
 1228 Laaksonen, A. (2021). The Arctic has warmed four times faster than the globe since 1980.
 1229 *Nature Portfolio*, (2022), 0–29. <https://doi.org/10.1038/s43247-022-00498-3>
- 1230 Raymond, P. A., McClelland, J. W., Holmes, R. M., Zhulidov, A. V., Mull, K., Peterson, B. J.,
 1231 ... Gurtovaya, T. Y. (2007). Flux and age of dissolved organic carbon exported to the Arctic

- 1232 Ocean: A carbon isotopic study of the five largest arctic rivers. *Global Biogeochemical*
1233 *Cycles*, 21(4). <https://doi.org/10.1029/2007GB002934>
- 1234 Ripley, B., Venables, B., Bates, D. M., Hornik, K., Gebhardt, A., & Firth, D. (2019). Package
1235 ‘MASS’ (Version 7.3-51.4). *Cran-R Project*.
- 1236 Schaefer, K., Lantuit, H., Romanovsky, V. E., Schuur, E. A. G., & Witt, R. (2014). The impact
1237 of the permafrost carbon feedback on global climate. *Environmental Research Letters*.
1238 <https://doi.org/10.1088/1748-9326/9/8/085003>
- 1239 Schuur, E. A. G., Abbott, B. W., Commane, R., Ernakovich, J., Euskirchen, E., Hugelius, G.,
1240 Grosse, G., Jones, M., Koven, C., Leshyk, V., Lawrence, D., Lorant, M. M., Mauritz, M.,
1241 Olefeldt, D., Natali, S., Rodenhizer, H., Salmon, V., Schädel, C., Strauss, J., ... Turetsky,
1242 M. (2022). Permafrost and climate change: Carbon cycle feedbacks from the warming
1243 arctic. *Annual Review of Environment and Resources*, 47, 343–371.
- 1244 Schuur, E. A. G., Bracho, R., Celis, G., Belshe, E. F., Ebert, C., Ledman, J., ... Webb, E. E.
1245 (2021). Tundra Underlain By Thawing Permafrost Persistently Emits Carbon to the
1246 Atmosphere Over 15 Years of Measurements. *Journal of Geophysical Research:*
1247 *Biogeosciences*, 126(6), 1–23. <https://doi.org/10.1029/2020jg006044>
- 1248 Schuur, T., McGuire, A. D., Romanovsky, V., Schädel, C., & Mack, M. (2018). Chapter 11:
1249 Arctic and Boreal Carbon. Second State of the Carbon Cycle Report. *Second State of the*
1250 *Carbon Cycle Report (SOCCR2): A Sustained Assessment Report*, 428–468. Retrieved from
1251 <https://carbon2018.globalchange.gov/chapter/11/>
- 1252 Selvam, B. P., Lapierre, J.-F., Guillemette, F., Voigt, C., Lamprecht, R. E., Biasi, C., ...
1253 Berggren, M. (2017). Degradation potentials of dissolved organic carbon (DOC) from
1254 thawed permafrost peat. *SCIENTIFIC REPORTS*, 7. <https://doi.org/10.1038/srep45811>
- 1255 Semenchuk, P. R., Elberling, B., Amtorp, C., Winkler, J., Rumpf, S., Michelsen, A., & Cooper,
1256 E. J. (2015). Deeper snow alters soil nutrient availability and leaf nutrient status in high
1257 Arctic tundra. *Biogeochemistry*, 124(1–3), 81–94. [https://doi.org/10.1007/s10533-015-](https://doi.org/10.1007/s10533-015-0082-7)
1258 [0082-7](https://doi.org/10.1007/s10533-015-0082-7)
- 1259 Shakil, S., Tank, S. E., Kokelj, S. V., Vonk, J. E., & Zolkos, S. (2020). Particulate dominance of
1260 organic carbon mobilization from thaw slumps on the Peel Plateau, NT: Quantification and
1261 implications for stream systems and permafrost carbon release. *Environmental Research*
1262 *Letters*, 15(11). <https://doi.org/10.1088/1748-9326/abac36>
- 1263 Sobek, S., Tranvik, L. J., Prairie, Y. T., Kortelainen, P., & Cole, J. J. (2007). Patterns and
1264 regulation of dissolved organic carbon: An analysis of 7,500 widely distributed lakes.
1265 *Limnology and Oceanography*, 52(3). <https://doi.org/10.4319/lo.2007.52.3.1208>
- 1266 Speetjens, N. J., Tanski, G., Martin, V., Wagner, J., Richter, A., Hugelius, G., ... Vonk, J. E.
1267 (2022). Dissolved organic matter characterization in soils and streams in a small coastal

- 1268 low-arctic catchment. *Biogeosciences*, 19(July), 3073–3097. Retrieved from
1269 <https://doi.org/10.5194/bg-19-3073-2022>
- 1270 Stolpmann, L., Coch, C., Morgenstern, A., Boike, J., Fritz, M., Herzsuh, U., ... Grosse, G.
1271 (2021). First pan-Arctic assessment of dissolved organic carbon in lakes of the permafrost
1272 region. *BIOGEOSCIENCES*, 18(12), 3917–3936. <https://doi.org/10.5194/bg-18-3917-2021>
- 1273 Strauss, J., Laboor, S., Schirrmeister, L., Fedorov, A. N., Fortier, D., Froese, D., ... Grosse, G.
1274 (2021). Circum-Arctic Map of the Yedoma Permafrost Domain. *Frontiers in Earth Science*,
1275 9. <https://doi.org/10.3389/feart.2021.758360>
- 1276 Striegl, R. G., Aiken, G. R., Dornblaser, M. M., Raymond, P. A., & Wickland, K. P. (2005). A
1277 decrease in discharge-normalized DOC export by the Yukon River during summer through
1278 autumn. *GEOPHYSICAL RESEARCH LETTERS*, 32(21).
1279 <https://doi.org/10.1029/2005GL024413>
- 1280 Tank, S. E., Frey, K. E., Striegl, R. G., Raymond, P. A., Holmes, R. M., McClelland, J. W., &
1281 Peterson, B. J. (2012). Landscape-level controls on dissolved carbon flux from diverse
1282 catchments of the circumboreal. *GLOBAL BIOGEOCHEMICAL CYCLES*, 26.
1283 <https://doi.org/10.1029/2012GB004299>
- 1284 Tanski, G., Wagner, D., Knoblauch, C., Fritz, M., Sachs, T., & Lantuit, H. (2019). Rapid CO2
1285 Release From Eroding Permafrost in Seawater. *Geophysical Research Letters*, 46(20).
1286 <https://doi.org/10.1029/2019GL084303>
- 1287 Tanski, George, Bröder, L., Wagner, D., Knoblauch, C., Lantuit, H., Beer, C., ... Vonk, J. E.
1288 (2021). Permafrost Carbon and CO2 Pathways Differ at Contrasting Coastal Erosion Sites
1289 in the Canadian Arctic. *Frontiers in Earth Science*, 9.
1290 <https://doi.org/10.3389/feart.2021.630493>
- 1291 Textor, S. R., Wickland, K. P., Podgorski, D. C., Johnston, S. E., & Spencer, R. G. M. (2019).
1292 Dissolved Organic Carbon Turnover in Permafrost-Influenced Watersheds of Interior
1293 Alaska: Molecular Insights and the Priming Effect. *FRONTIERS IN EARTH SCIENCE*, 7.
1294 <https://doi.org/10.3389/feart.2019.00275>
- 1295 Tfaily, M. M., Hamdan, R., Corbett, J. E., Chanton, J. P., Glaser, P. H., & Cooper, W. T. (2013).
1296 Investigating dissolved organic matter decomposition in northern peatlands using
1297 complimentary analytical techniques. *Geochimica et Cosmochimica Acta*.
1298 <https://doi.org/10.1016/j.gca.2013.03.002>
- 1299 Thurman, E. M. (1985). Organic geochemistry of natural waters (Vol. 2). Springer Science &
1300 Business Media.
- 1301 Treat, C. C., Jones, M. C., Camill, P., Gallego-Sala, A., Garneau, M., Harden, J. W., ...
1302 Väiliranta, M. (2016). Effects of permafrost aggradation on peat properties as determined
1303 from a pan-Arctic synthesis of plant macrofossils. *Journal of Geophysical Research*:

- 1304 *Biogeosciences*, 121(1), 78–94. <https://doi.org/10.1002/2015JG003061>
- 1305 Treat, Claire C., & Jones, M. C. (2018). Near-surface permafrost aggradation in Northern
1306 Hemisphere peatlands shows regional and global trends during the past 6000 years.
1307 *Holocene*. <https://doi.org/10.1177/0959683617752858>
- 1308 Turetsky, M. R., Wieder, R. K., Vitt, D. H., Evans, R. J., & Scott, K. D. (2007). The
1309 disappearance of relict permafrost in boreal north America: Effects on peatland carbon
1310 storage and fluxes. *Global Change Biology*, 13(9), 1922–1934.
1311 <https://doi.org/10.1111/j.1365-2486.2007.01381.x>
- 1312 Turetsky, Merritt R., Abbott, B. W., Jones, M. C., Anthony, K. W., Olefeldt, D., Schuur, E. A.
1313 G., ... McGuire, A. D. (2020). Carbon release through abrupt permafrost thaw. *Nature*
1314 *Geoscience*. <https://doi.org/10.1038/s41561-019-0526-0>
- 1315 USDA. (1999). *Soil Taxonomy: A Basic System of Soil Classification for Making and*
1316 *Interpreting Soil Surveys, 2nd Edition. Landscape and Land Capacity.*
- 1317 Varner, R. K., Crill, P. M., Frohking, S., McCalley, C. K., Burke, S. A., Chanton, J. P., ... Palace,
1318 M. W. (2022). Permafrost thaw driven changes in hydrology and vegetation cover increase
1319 trace gas emissions and climate forcing in Stordalen Mire from 1970 to 2014. *Philosophical*
1320 *Transactions of the Royal Society A: Mathematical, Physical and Engineering Sciences*,
1321 380(2215). <https://doi.org/10.1098/rsta.2021.0022>
- 1322 Vonk, J E, Tank, S. E., Mann, P. J., Spencer, R. G. M., Treat, C. C., Striegl, R. G., ... Wickland,
1323 K. P. (2015). Biodegradability of dissolved organic carbon in permafrost soils and aquatic
1324 systems: a meta-analysis. *BIOGEOSCIENCES*, 12(23), 6915–6930.
1325 <https://doi.org/10.5194/bg-12-6915-2015>
- 1326 Vonk, Jorien E., & Gustafsson, Ö. (2013). Permafrost-carbon complexities. *Nature Geoscience*.
1327 <https://doi.org/10.1038/ngeo1937>
- 1328 Vonk, J. E., Mann, P. J., Davydov, S., Davydova, A., Spencer, R. G. M., Schade, J., ... Holmes,
1329 R. M. (2013). High biolability of ancient permafrost carbon upon thaw. *GEOPHYSICAL*
1330 *RESEARCH LETTERS*, 40(11), 2689–2693. <https://doi.org/10.1002/grl.50348>
- 1331 Wang JA, Sulla-Menashe D, Woodcock CE, Sonnentag O, Keeling RF, Friedl MA. Extensive
1332 land cover change across Arctic–Boreal Northwestern North America from disturbance and
1333 climate forcing. *Glob Change Biol*. 2020; 26: 807–822. <https://doi.org/10.1111/gcb.14804>
- 1334 Weishaar, J. L., Aiken, G. R., Bergamaschi, B. A., Fram, M. S., Fujii, R., & Mopper, K. (2003).
1335 Evaluation of specific ultraviolet absorbance as an indicator of the chemical composition
1336 and reactivity of dissolved organic carbon. *Environmental Science and Technology*, 37(20),
1337 4702–4708. <https://doi.org/10.1021/es030360x>
- 1338 Weyhenmeyer, G. A., Fröberg, M., Karlton, E., Khalili, M., Kothawala, D., Temnerud, J., &

- 1339 Tranvik, L. J. (2012). Selective decay of terrestrial organic carbon during transport from
1340 land to sea. *Global Change Biology*, 18(1). [https://doi.org/10.1111/j.1365-](https://doi.org/10.1111/j.1365-2486.2011.02544.x)
1341 [2486.2011.02544.x](https://doi.org/10.1111/j.1365-2486.2011.02544.x)
- 1342 Wickland, K.P., Neff, J. C., & Aiken, G. R. (2007). Dissolved organic carbon in Alaskan boreal
1343 forest: Sources, chemical characteristics, and biodegradability. *Ecosystems*, 10(8), 1323–
1344 1340. <https://doi.org/10.1007/s10021-007-9101-4>
- 1345 Wickland, Kimberly P, Waldrop, M. P., Aiken, G. R., Koch, J. C., Jorgenson, Mt., & Striegl, R.
1346 G. (2018). Dissolved organic carbon and nitrogen release from boreal Holocene permafrost
1347 and seasonally frozen soils of Alaska. *ENVIRONMENTAL RESEARCH LETTERS*, 13(6).
1348 <https://doi.org/10.1088/1748-9326/aac4ad>
- 1349 Wild, B., Andersson, A., Broder, L., Vonk, J., Hugelius, G., McClelland, J. W., ... Gustafsson,
1350 O. (2019). Rivers across the Siberian Arctic unearth the patterns of carbon release from
1351 thawing permafrost. *PROCEEDINGS OF THE NATIONAL ACADEMY OF SCIENCES OF*
1352 *THE UNITED STATES OF AMERICA*, 116(21), 10280–10285.
1353 <https://doi.org/10.1073/pnas.1811797116>
- 1354 Wild, B., Gentsch, N., Capek, P., Diáková, K., Alves, R. J. E., Bárta, J., ... Richter, A. (2016).
1355 Plant-derived compounds stimulate the decomposition of organic matter in arctic permafrost
1356 soils. *Scientific Reports*, 6. <https://doi.org/10.1038/srep25607>
- 1357 Wild, B., Schnecker, J., Bárta, J., Čapek, P., Guggenberger, G., Hofhansl, F., ... Richter, A.
1358 (2013). Nitrogen dynamics in Turbic Cryosols from Siberia and Greenland. *Soil Biology*
1359 *and Biochemistry*, 67, 85–93. <https://doi.org/https://doi.org/10.1016/j.soilbio.2013.08.004>
- 1360 Woo, M. (1986). Permafrost hydrology in north america. *Atmosphere - Ocean*, 24(3).
1361 <https://doi.org/10.1080/07055900.1986.9649248>
- 1362
- 1363
- 1364
- 1365
- 1366
- 1367
- 1368
- 1369

1370

1371

1372 **Studies used to generate database**

1373 Abbott, B. W., Jones, J. B., Godsey, S. E., Larouche, J. R., & Bowden, W. B. (2015). Patterns
1374 and persistence of hydrologic carbon and nutrient export from collapsing upland permafrost.
1375 *Biogeosciences*, *12*(12), 3725–3740. <https://doi.org/10.5194/bg-12-3725-2015>

1376 Abbott, B. W., Larouche, J. R., Jones, J. J. B., Bowden, W. B., & Balser, A. W. (2014). From
1377 Thawing and Collapsing Permafrost. *Journal of Geophysical Research: Biogeosciences*,
1378 *119*, 2049–2063. <https://doi.org/10.1002/2014JG002678>.Received

1379 Beckebanze, L., Runkle, B. R. K., Walz, J., Wille, C., Holl, D., Helbig, M., ... Kutzbach, L.
1380 (2022). Lateral carbon export has low impact on the net ecosystem carbon balance of a
1381 polygonal tundra catchment. *BIOGEOSCIENCES*, *19*(16), 3863–3876.
1382 <https://doi.org/10.5194/bg-19-3863-2022>

1383 Boddy, E., Roberts, P., Hill, P. W., Farrar, J., & Jones, D. L. (2008). Turnover of low molecular
1384 weight dissolved organic C (DOC) and microbial C exhibit different temperature
1385 sensitivities in Arctic tundra soils. *SOIL BIOLOGY & BIOCHEMISTRY*, *40*(7), 1557–1566.
1386 <https://doi.org/10.1016/j.soilbio.2008.01.030>

1387 Bristol, E. M., Connolly, C. T., Lorenson, T. D., Richmond, B. M., Ilgen, A. G., Choens, R. C.,
1388 ... McClelland, J. W. (2021). Geochemistry of Coastal Permafrost and Erosion-Driven
1389 Organic Matter Fluxes to the Beaufort Sea Near Drew Point, Alaska. *Frontiers in Earth
1390 Science*, *8*. <https://doi.org/10.3389/feart.2020.598933>

1391 Bruhn, A. D., Stedmon, C. A., Comte, J., Matsuoka, A., Speetjens, N. J., Tanski, G., ... Sjöstedt,
1392 J. (2021). Terrestrial Dissolved Organic Matter Mobilized From Eroding Permafrost
1393 Controls Microbial Community Composition and Growth in Arctic Coastal Zones.
1394 *Frontiers in Earth Science*, *9*. <https://doi.org/10.3389/feart.2021.640580>

1395 Buckeridge, K. M., & Grogan, P. (2008). Deepened snow alters soil microbial nutrient
1396 limitations in arctic birch hummock tundra. *Applied Soil Ecology*, *39*(2), 210–222.
1397 <https://doi.org/https://doi.org/10.1016/j.apsoil.2007.12.010>

1398 Burd, K., Estop-Aragónés, C., Tank, S. E., & Olefeldt, D. (2020). Lability of dissolved organic
1399 carbon from boreal peatlands: interactions between permafrost thaw, wildfire, and season.
1400 *Canadian Journal of Soil Science*, *13*(February), 1–13. <https://doi.org/10.1139/cjss-2019-0154>
1401

1402 Burd, K., Tank, S. E., Dion, N., Quinton, W. L., Spence, C., Tanentzap, A. J., & Olefeldt, D.
1403 (2018). Seasonal shifts in export of DOC and nutrients from burned and unburned peatland-

- 1404 rich catchments, Northwest Territories, Canada. *Hydrology and Earth System Sciences*,
1405 4455–4472. <https://doi.org/10.5194/hess-22-4455-2018>
- 1406 Carey, S. K. (2003). Dissolved organic carbon fluxes in a discontinuous permafrost subarctic
1407 alpine catchment. *PERMAFROST AND PERIGLACIAL PROCESSES*, 14(2), 161–171.
1408 <https://doi.org/10.1002/ppp.444>
- 1409 Chiasson-Poirier, G., Franssen, J., Lafreniere, M. J., Fortier, D., & Lamoureux, S. F. (2020).
1410 Seasona evolution of active layer thaw depth and hillslope-stream connectivity in a
1411 permafrost watershed. *WATER RESOURCES RESEARCH*, 56(1).
1412 <https://doi.org/10.1029/2019WR025828>
- 1413 Connolly, C. T., Cardenas, M. B., Burkart, G. A., Spencer, R. G. M., & McClelland, J. W.
1414 (2020). Groundwater as a major source of dissolved organic matter to Arctic coastal waters.
1415 *NATURE COMMUNICATIONS*, 11(1). <https://doi.org/10.1038/s41467-020-15250-8>
- 1416 Cory, R. M., Crump, B. C., Dobkowski, J. A., & Kling, G. W. (2013). Surface exposure to
1417 sunlight stimulates CO₂ release from permafrost soil carbon in the Arctic. *Proceedings of*
1418 *the National Academy of Sciences*, 110(9), 3429–3434.
1419 <https://doi.org/10.1073/pnas.1214104110>
- 1420 Deshpande, B. N., Crevecoeur, S., Matveev, A., & Vincent, W. F. (2016). Bacterial production
1421 in subarctic peatland lakes enriched by thawing permafrost. *BIOGEOSCIENCES*, 13(15),
1422 4411–4427. <https://doi.org/10.5194/bg-13-4411-2016>
- 1423 Douglas, T. A., Fortier, D., Shur, Y. L., Kanevskiy, M. Z., Guo, L., Cai, Y., & Bray, M. T.
1424 (2011). Biogeochemical and Geocryological Characteristics of Wedge and Thermokarst-
1425 Cave Ice in the CRREL Permafrost Tunnel, Alaska. *PERMAFROST AND PERIGLACIAL*
1426 *PROCESSES*, 22(2), 120–128. <https://doi.org/10.1002/ppp.709>
- 1427 Drake, T. W., Wickland, K. P., Spencer, R. G. M., McKnight, D. M., & Striegl, R. G. (2015).
1428 Ancient low-molecular-weight organic acids in permafrost fuel rapid carbon dioxide
1429 production upon thaw. *PROCEEDINGS OF THE NATIONAL ACADEMY OF SCIENCES*
1430 *OF THE UNITED STATES OF AMERICA*, 112(45), 13946–13951.
1431 <https://doi.org/10.1073/pnas.1511705112>
- 1432 Dutta, K., Schuur, E. A. G., Neff, J. C., & Zimov, S. A. (2006). Potential carbon release from
1433 permafrost soils of Northeastern Siberia. *GLOBAL CHANGE BIOLOGY*, 12(12), 2336–
1434 2351. <https://doi.org/10.1111/j.1365-2486.2006.01259.x>
- 1435 Edwards, K. A., & Jefferies, R. L. (2013). Inter-annual and seasonal dynamics of soil microbial
1436 biomass and nutrients in wet and dry low-Arctic sedge meadows. *Soil Biology and*
1437 *Biochemistry*, 57, 83–90. <https://doi.org/https://doi.org/10.1016/j.soilbio.2012.07.018>
- 1438 Edwards, K. A., McCulloch, J., Kershaw], G. [Peter, & Jefferies, R. L. (2006). Soil microbial
1439 and nutrient dynamics in a wet Arctic sedge meadow in late winter and early spring. *Soil*

- 1440 *Biology and Biochemistry*, 38(9), 2843–2851.
 1441 <https://doi.org/https://doi.org/10.1016/j.soilbio.2006.04.042>
- 1442 Ernakovich, J. G., Lynch, L. M., Brewer, P. E., Calderon, F. J., & Wallenstein, M. D. (2017).
 1443 Redox and temperature-sensitive changes in microbial communities and soil chemistry
 1444 dictate greenhouse gas loss from thawed permafrost. *BIOGEOCHEMISTRY*, 134(1–2),
 1445 183–200. <https://doi.org/10.1007/s10533-017-0354-5>
- 1446 Ewing, S. A., Paces, J. B., O'Donnell, J. A., Jorgenson, M. T., Kanevskiy, M. Z., Aiken, G. R.,
 1447 ... Striegl, R. (2015). Uranium isotopes and dissolved organic carbon in loess permafrost:
 1448 Modeling the age of ancient ice. *GEOCHIMICA ET COSMOCHIMICA ACTA*, 152, 143–
 1449 165. <https://doi.org/10.1016/j.gca.2014.11.008>
- 1450 Fenger-Nielsen, R., Hollesen, J., Matthiesen, H., Andersen, E. A. S., Westergaard-Nielsen, A.,
 1451 Harmsen, H., ... Elberling, B. (2019). Footprints from the past: The influence of past human
 1452 activities on vegetation and soil across five archaeological sites in Greenland. *Science of the*
 1453 *Total Environment*, 654, 895–905. <https://doi.org/10.1016/j.scitotenv.2018.11.018>
- 1454 Fouché, J., Christiansen, C. T., Lafrenière, M. J., Grogan, P., & Lamoureux, S. F. (2020).
 1455 Canadian permafrost stores large pools of ammonium and optically distinct
 1456 dissolved organic matter. *Nature Communications*, 11(1), 4500.
 1457 <https://doi.org/10.1038/s41467-020-18331-w>
- 1458 Fouche, J., Bouchez, C., Keller, C., Allard, M., & Ambrosi, J.-P. (2021). Seasonal cryogenic
 1459 processes control supra-permafrost pore water chemistry in two contrasting Cryosols.
 1460 *GEODERMA*, 401. <https://doi.org/10.1016/j.geoderma.2021.115302>
- 1461 Fouché, J., Keller, C., Allard, M., Ambrosi, J. P., Fouche, J., Keller, C., ... Ambrosi, J. P. (2014).
 1462 Increased CO₂ fluxes under warming tests and soil solution chemistry in Histic and Turbic
 1463 Cryosols, Salluit, Nunavik, Canada. *Soil Biology and Biochemistry*, 68, 185–199.
 1464 <https://doi.org/https://doi.org/10.1016/j.soilbio.2013.10.007>
- 1465 Fritz, M., Opel, T., Tanski, G., Herzsuh, U., Meyer, H., Eulenburg, A., & Lantuit, H. (2015).
 1466 Dissolved organic carbon (DOC) in Arctic ground ice. *CRYOSPHERE*, 9(2), 737–752.
 1467 <https://doi.org/10.5194/tc-9-737-2015>
- 1468 Gagné, K. R., Ewers, S. C., Murphy, C. J., Daanen, R., Walter Anthony, K., & Guerard, J. J.
 1469 (2020). Composition and photo-reactivity of organic matter from permafrost soils and
 1470 surface waters in interior Alaska. *Environmental Science: Processes and Impacts*, 22(7),
 1471 1525–1539. <https://doi.org/10.1039/d0em00097c>
- 1472 Gao, L., Zhou, Z., Reyes V, A., & Guo, L. (2018). Yields and Characterization of Dissolved
 1473 Organic Matter From Different Aged Soils in Northern Alaska. *JOURNAL OF*
 1474 *GEOPHYSICAL RESEARCH-BIOGEOSCIENCES*, 123(7), 2035–2052.
 1475 <https://doi.org/10.1029/2018JG004408>

- 1476 Herndon, E. M., Mann, B. F., Chowdhury, T. R., Yang, Z., Wullschleger, S. D., Graham, D., ...
 1477 Gu, B. (2015). Pathways of anaerobic organic matter decomposition in tundra soils from
 1478 Barrow, Alaska. *JOURNAL OF GEOPHYSICAL RESEARCH-BIOGEOSCIENCES*,
 1479 *120*(11), 2345–2359. <https://doi.org/10.1002/2015JG003147>
- 1480 Herndon, E. M., Yang, Z., Bargar, J., Janot, N., Regier, T. Z., Graham, D. E., ... Liang, L.
 1481 (2015). Geochemical drivers of organic matter decomposition in arctic tundra soils.
 1482 *BIOGEOCHEMISTRY*, *126*(3), 397–414. <https://doi.org/10.1007/s10533-015-0165-5>
- 1483 Herndon, E., AlBashaireh, A., Singer, D., Chowdhury, T. [Roy, Gu, B., & Graham, D. (2017).
 1484 Influence of iron redox cycling on organo-mineral associations in Arctic tundra soil.
 1485 *Geochimica et Cosmochimica Acta*, *207*, 210–231.
 1486 <https://doi.org/https://doi.org/10.1016/j.gca.2017.02.034>
- 1487 Heslop, J. K., Chandra, S., Sobczak, W. V., Davydov, S. P., Davydova, A. I., Spektor, V. V., &
 1488 Anthony, K. M. W. (2017). Variable respiration rates of incubated permafrost soil extracts
 1489 from the Kolyma River lowlands, north-east Siberia. *POLAR RESEARCH*, *36*.
 1490 <https://doi.org/10.1080/17518369.2017.1305157>
- 1491 Hirst, C., Mauclet, E., Monhonval, A., Tihon, E., Ledman, J., Schuur, E. A. G., & Opfergelt, S.
 1492 (2022). Seasonal Changes in Hydrology and Permafrost Degradation Control Mineral
 1493 Element-Bound DOC Transport From Permafrost Soils to Streams. *GLOBAL*
 1494 *BIOGEOCHEMICAL CYCLES*, *36*(2). <https://doi.org/10.1029/2021GB007105>
- 1495 Hodgkins, S. B., Tfaily, M. M., Podgorski, D. C., McCalley, C. K., Saleska, S. R., Crill, P. M.,
 1496 ... Cooper, W. T. (2016). Elemental composition and optical properties reveal changes in
 1497 dissolved organic matter along a permafrost thaw chronosequence in a subarctic peatland.
 1498 *Geochimica et Cosmochimica Acta*, *187*, 123–140.
 1499 <https://doi.org/10.1016/j.gca.2016.05.015>
- 1500 Jilkova, V., Devetter, M., Bryndova, M., Hajek, T., Kotas, P., Lulakova, P., ... Macek, P. (2021).
 1501 Carbon Sequestration Related to Soil Physical and Chemical Properties in the High Arctic.
 1502 *GLOBAL BIOGEOCHEMICAL CYCLES*, *35*(9). <https://doi.org/10.1029/2020GB006877>
- 1503 Kane, E. S., Chivers, M. R., Turetsky, M. R., Treat, C. C., Petersen, D. G., Waldrop, M., ...
 1504 McGuire, A. D. (2013). Response of anaerobic carbon cycling to water table manipulation
 1505 in an Alaskan rich fen. *Soil Biology and Biochemistry*, *58*, 50–60.
 1506 <https://doi.org/https://doi.org/10.1016/j.soilbio.2012.10.032>
- 1507 Kane, E. S., Valentine, D. W., Michaelson, G. J., Fox, J. D., & Ping, C.-L. (2006). Controls over
 1508 pathways of carbon efflux from soils along climate and black spruce productivity gradients
 1509 in interior Alaska. *Soil Biology and Biochemistry*, *38*(6), 1438–1450.
 1510 <https://doi.org/https://doi.org/10.1016/j.soilbio.2005.11.004>
- 1511 Kane, E. S., Turetsky, M. R., Harden, J. W., McGuire, A. D., & Waddington, J. M. (2010).
 1512 Seasonal ice and hydrologic controls on dissolved organic carbon and nitrogen

- 1513 concentrations in a boreal-rich fen. *JOURNAL OF GEOPHYSICAL RESEARCH-*
1514 *BIOGEOSCIENCES*, 115. <https://doi.org/10.1029/2010JG001366>
- 1515 Kawahigashi, M., Prokushkin, A., & Sumida, H. (2011). Effect of fire on solute release from
1516 organic horizons under larch forest in Central Siberian permafrost terrain. *Geoderma*,
1517 166(1), 171–180. <https://doi.org/https://doi.org/10.1016/j.geoderma.2011.07.027>
- 1518 Koch, J. C., Runkel, R. L., Striegl, R., & McKnight, D. M. (2013). Hydrologic controls on the
1519 transport and cycling of carbon and nitrogen in a boreal catchment underlain by continuous
1520 permafrost. *JOURNAL OF GEOPHYSICAL RESEARCH-BIOGEOSCIENCES*, 118(2),
1521 698–712. <https://doi.org/10.1002/jgrg.20058>
- 1522 Lim, A. G., Loiko, S. V, Kuzmina, D. M., Krickov, I. V, Shirokova, L. S., Kulizhsky, S. P., ...
1523 Pokrovsky, O. S. (2021). Dispersed ground ice of permafrost peatlands: Potential
1524 unaccounted carbon, nutrient and metal sources. *Chemosphere*, 266, 128953.
1525 <https://doi.org/10.1016/j.chemosphere.2020.128953>
- 1526 Lindborg, T., Rydberg, J., Tröjbom, M., Berglund, S., Johansson, E., Löfgren, A., ... Laudon, H.
1527 (2016). Biogeochemical data from terrestrial and aquatic ecosystems in a periglacial
1528 catchment, West Greenland. *Earth System Science Data*, 8(2), 439–459.
1529 <https://doi.org/10.5194/essd-8-439-2016>
- 1530 Littlefair, C. A., & Tank, S. E. (2018). Biodegradability of Thermokarst Carbon in a Till-
1531 Associated, Glacial Margin Landscape: The Case of the Peel Plateau, NWT, Canada.
1532 *JOURNAL OF GEOPHYSICAL RESEARCH-BIOGEOSCIENCES*, 123(10), 3293–3307.
1533 <https://doi.org/10.1029/2018JG004461>
- 1534 Liu, N., Michelsen, A., & Rinnan, R. (2020). Vegetation and soil responses to added carbon and
1535 nutrients remain six years after discontinuation of long-term treatments. *Science of the Total*
1536 *Environment*, 722, 137885. <https://doi.org/10.1016/j.scitotenv.2020.137885>
- 1537 Loiko, S. V, Pokrovsky, O. S., Raudina, T. V, Lim, A., Kolesnichenko, L. G., Shirokova, L. S.,
1538 ... Kirpotin, S. N. (2017). Abrupt permafrost collapse enhances organic carbon, CO₂,
1539 nutrient and metal release into surface waters. *Chemical Geology*, 471, 153–165.
1540 <https://doi.org/https://doi.org/10.1016/j.chemgeo.2017.10.002>
- 1541 MacDonald, E. N., Tank, S. E., Kokelj, S. V., Froese, D. G., & Hutchins, R. H. S. (2021).
1542 Permafrost-derived dissolved organic matter composition varies across permafrost end-
1543 members in the western Canadian Arctic. *Environmental Research Letters*, 16(2).
1544 <https://doi.org/10.1088/1748-9326/abd971>
- 1545 Mangal, V., DeGasparro, S., Beresford, D. V, & Guéguen, C. (2020). Linking molecular and
1546 optical properties of dissolved organic matter across a soil-water interface on Akimiski
1547 Island (Nunavut, Canada). *Science of The Total Environment*, 704, 135415.
1548 <https://doi.org/https://doi.org/10.1016/j.scitotenv.2019.135415>

- 1549 Masyagina, O. V, Tokareva, I. V, & Prokushkin, A. S. (2016). Post fire organic matter
 1550 biodegradation in permafrost soils: Case study after experimental heating of mineral
 1551 horizons. *Science of The Total Environment*, 573, 1255–1264.
 1552 <https://doi.org/https://doi.org/10.1016/j.scitotenv.2016.04.195>
- 1553 McFarlane, K. J., Throckmorton, H. M., Heikoop, J. M., Newman, B. D., Hedgpeth, A. L.,
 1554 Repasch, M. N., ... Wilson, C. J. (2022). Age and chemistry of dissolved organic carbon
 1555 reveal enhanced leaching of ancient labile carbon at the permafrost thaw zone.
 1556 *BIOGEOSCIENCES*, 19(4), 1211–1223. <https://doi.org/10.5194/bg-19-1211-2022>
- 1557 Mörsdorf, M. A., Baggesen, N. S., Yoccoz, N. G., Michelsen, A., Elberling, B., Ambus, P. L., &
 1558 Cooper, E. J. (2019). Deepened winter snow significantly influences the availability and
 1559 forms of nitrogen taken up by plants in High Arctic tundra. *Soil Biology and Biochemistry*,
 1560 135, 222–234. <https://doi.org/https://doi.org/10.1016/j.soilbio.2019.05.009>
- 1561 Neff, J. C., & Hooper, D. U. (2002). Vegetation and climate controls on potential CO₂, DOC and
 1562 DON production in northern latitude soils. *Global Change Biology*, 8(9), 872–884.
 1563 <https://doi.org/10.1046/j.1365-2486.2002.00517.x>
- 1564 Nielsen, C. S., Michelsen, A., Strobel, B. W., Wulff, K., Banyasz, I., & Elberling, B. (2017).
 1565 Correlations between substrate availability, dissolved CH₄, and CH₄ emissions in an arctic
 1566 wetland subject to warming and plant removal. *JOURNAL OF GEOPHYSICAL*
 1567 *RESEARCH-BIOGEOSCIENCES*, 122(3), 645–660. <https://doi.org/10.1002/2016JG003511>
- 1568 O'Donnell, J. A., Aiken, G. R., Butler, K. D., Guillemette, F., Podgorski, D. C., & Spencer, R.
 1569 G. M. (2016). DOM composition and transformation in boreal forest soils: The effects of
 1570 temperature and organic-horizon decomposition state. *JOURNAL OF GEOPHYSICAL*
 1571 *RESEARCH-BIOGEOSCIENCES*, 121(10), 2727–2744.
 1572 <https://doi.org/10.1002/2016JG003431>
- 1573 O'Donnell, J. A., Turetsky, M. R., Harden, J. W., Manies, K. L., Pruett, L. E., Shetler, G., &
 1574 Neff, J. C. (2009). Interactive Effects of Fire, Soil Climate, and Moss on CO₂ Fluxes in
 1575 Black Spruce Ecosystems of Interior Alaska. *ECOSYSTEMS*, 12(1), 57–72.
 1576 <https://doi.org/10.1007/s10021-008-9206-4>
- 1577 Oiffer, L., & Siciliano, S. D. (2009). Methyl mercury production and loss in Arctic soil. *Science*
 1578 *of the Total Environment*, 407(5), 1691–1700.
 1579 <https://doi.org/10.1016/j.scitotenv.2008.10.025>
- 1580 Olefeldt, D., & Roulet, N. T. (2012). Effects of permafrost and hydrology on the composition
 1581 and transport of dissolved organic carbon in a subarctic peatland complex. *Journal of*
 1582 *Geophysical Research: Biogeosciences*, 117(1). <https://doi.org/10.1029/2011JG001819>
- 1583 Olefeldt, D., & Roulet, N. T. (2014). Permafrost conditions in peatlands regulate magnitude,
 1584 timing, and chemical composition of catchment dissolved organic carbon export. *Global*
 1585 *Change Biology*, 20(10), 3122–3136. <https://doi.org/10.1111/gcb.12607>

- 1586 Olefeldt, D., Roulet, N. T., Bergeron, O., Crill, P., Bäckstrand, K., & Christensen, T. R. (2012).
 1587 Net carbon accumulation of a high-latitude permafrost tundra mire similar to permafrost-free
 1588 peatlands. *Geophysical Research Letters*. <https://doi.org/10.1029/2011GL050355>
- 1589 Olsrud, M., & Christensen, T. R. (2011). Carbon partitioning in a wet and a semiwet subarctic
 1590 mire ecosystem based on in situ ¹⁴C pulse-labelling. *Soil Biology and Biochemistry*, *43*(2),
 1591 231–239. <https://doi.org/10.1016/j.soilbio.2010.09.034>
- 1592 Pastor, A., Poblador, S., Skovsholt, L. J., & Riis, T. (2020). Microbial carbon and nitrogen
 1593 processes in high-Arctic riparian soils. *PERMAFROST AND PERIGLACIAL PROCESSES*,
 1594 *31*(1), 223–236. <https://doi.org/10.1002/ppp.2039>
- 1595 Patzner, M. S., Mueller, C. W., Malusova, M., Baur, M., Nikeleit, V., Scholten, T., ... Bryce, C.
 1596 (2020). Iron mineral dissolution releases iron and associated organic carbon during
 1597 permafrost thaw. *Nature Communications*, *11*(1), 1–11. [https://doi.org/10.1038/s41467-020-](https://doi.org/10.1038/s41467-020-20102-6)
 1598 [20102-6](https://doi.org/10.1038/s41467-020-20102-6)
- 1599 Patzner, M. S., Logan, M., McKenna, A. M., Young, R. B., Zhou, Z., Joss, H., ... Bryce, C.
 1600 (2022). Microbial iron cycling during tundra hillslope collapse promotes greenhouse gas
 1601 emissions before complete permafrost thaw. *Communications Earth & Environment*, *3*(1),
 1602 76. <https://doi.org/10.1038/s43247-022-00407-8>
- 1603 Payandi-Rolland, D., Shirokova, L. S., Tesfa, M., Bénézeth, P., Lim, A. G., Kuzmina, D., ...
 1604 Pokrovsky, O. S. (2020). Dissolved organic matter biodegradation along a hydrological
 1605 continuum in permafrost peatlands. *Science of The Total Environment*, *749*, 141463.
 1606 <https://doi.org/10.1016/J.SCITOTENV.2020.141463>
- 1607 Payandi-Rolland, D., Shirokova, L. S., Labonne, F., Bénézeth, P., & Pokrovsky, O. S. (2021).
 1608 Impact of freeze-thaw cycles on organic carbon and metals in waters of
 1609 permafrost peatlands. *Chemosphere*, *279*, 130510.
 1610 <https://doi.org/10.1016/j.chemosphere.2021.130510>
- 1611 Payandi-Rolland, D., Shirokova, L. S., Nakhle, P., Tesfa, M., Abdou, A., Causserand, C., ...
 1612 Pokrovsky, O. S. (2020). Aerobic release and biodegradation of dissolved organic matter
 1613 from frozen peat: Effects of temperature and heterotrophic bacteria. *CHEMICAL*
 1614 *GEOLOGY*, *536*. <https://doi.org/10.1016/j.chemgeo.2019.119448>
- 1615 Petersen, D. G., Blazewicz, S. J., Firestone, M., Herman, D. J., Turetsky, M., & Waldrop, M.
 1616 (2012). Abundance of microbial genes associated with nitrogen cycling as indices of
 1617 biogeochemical process rates across a vegetation gradient in Alaska. *Environmental*
 1618 *Microbiology*, *14*(4), 993–1008. <https://doi.org/10.1111/j.1462-2920.2011.02679.x>
- 1619 Pokrovsky, O. S., Reynolds, B. C., Prokushkin, A. S., Schott, J., & Viers, J. (2013). Silicon
 1620 isotope variations in Central Siberian rivers during basalt weathering in permafrost-
 1621 dominated larch forests. *Chemical Geology*, *355*, 103–116.
 1622 <https://doi.org/10.1016/j.chemgeo.2013.07.016>

- 1623 Pokrovsky, O. S., Schott, J., Kudryavtzev, D. I., & Dupré, B. (2005). Basalt weathering in
 1624 Central Siberia under permafrost conditions. *Geochimica et Cosmochimica Acta*, 69(24),
 1625 5659–5680. <https://doi.org/10.1016/j.gca.2005.07.018>
- 1626 Pokrovsky, O. S., Manasypov, R. M., Loiko, S. V., & Shirokova, L. S. (2016). Organic and
 1627 organo-mineral colloids in discontinuous permafrost zone. *Geochimica et Cosmochimica*
 1628 *Acta*, 188, 1–20. <https://doi.org/https://doi.org/10.1016/j.gca.2016.05.035>
- 1629 Poulin, B. A., Ryan, J. N., Tate, M. T., Krabbenhoft, D. P., Hines, M. E., Barkay, T., ... Aiken,
 1630 G. R. (2019). Geochemical Factors Controlling Dissolved Elemental Mercury and
 1631 Methylmercury Formation in Alaskan Wetlands of Varying Trophic Status. *Environmental*
 1632 *Science and Technology*, 53(11), 6203–6213. <https://doi.org/10.1021/acs.est.8b06041>
- 1633 Prokushkin, A. S., Gavrilenko, I. V., Abaimov, A. P., Prokushkin, S. G., & Samusenko, A. V.
 1634 (2006). Dissolved organic carbon in upland forested watersheds underlain by continuous
 1635 permafrost in Central Siberia. *Mitigation and Adaptation Strategies for Global Change*,
 1636 11(1), 223–240. <https://doi.org/10.1007/s11027-006-1022-6>
- 1637 Prokushkin, A. S., Gleixner, G., McDowell, W. H., Ruehlow, S., & Schulze, E.-D. (2007).
 1638 Source- and substrate-specific export of dissolved organic matter from permafrost-
 1639 dominated forested watershed in central Siberia. *GLOBAL BIOGEOCHEMICAL CYCLES*,
 1640 21(4). <https://doi.org/10.1029/2007GB002938>
- 1641 Prokushkin, A. S., Kajimoto, T., Prokushkin, S. G., McDowell, W. H., Abaimov, A. P., &
 1642 Matsuura, Y. (2005). Climatic factors influencing fluxes of dissolved organic carbon from
 1643 the forest floor in a continuous-permafrost Siberian watershed. *CANADIAN JOURNAL OF*
 1644 *FOREST RESEARCH*, 35(9), 2130–2140. <https://doi.org/10.1139/X05-150>
- 1645 Rasmussen, L. H., Michelsen, A., Ladegaard-Pedersen, P., Nielsen, C. S., & Elberling, B.
 1646 (2020). Arctic soil water chemistry in dry and wet tundra subject to snow addition, summer
 1647 warming and herbivory simulation. *Soil Biology and Biochemistry*, 141, 107676.
 1648 <https://doi.org/https://doi.org/10.1016/j.soilbio.2019.107676>
- 1649 Raudina, T. V., Loiko, S. V., Lim, A., Manasypov, R. M., Shirokova, L. S., Istigechev, G. I., ...
 1650 Pokrovsky, O. S. (2018). Permafrost thaw and climate warming may decrease the CO₂,
 1651 carbon, and metal concentration in peat soil waters of the Western Siberia Lowland. *Science*
 1652 *of The Total Environment*, 634, 1004–1023.
 1653 <https://doi.org/https://doi.org/10.1016/j.scitotenv.2018.04.059>
- 1654 Raudina, T. V., Loiko, S. V., Lim, A. G., Krickov, I. V., Shirokova, L. S., Istigechev, G. I., ...
 1655 Pokrovsky, O. S. (2017). Dissolved organic carbon and major and trace elements in peat
 1656 porewater of sporadic, discontinuous, and continuous permafrost zones of western Siberia.
 1657 *BIOGEOSCIENCES*, 14(14), 3561–3584. <https://doi.org/10.5194/bg-14-3561-2017>

- 1658 Ro, H.-M., Ji, Y., & Lee, B. (2018). Interactive effect of soil moisture and temperature regimes
1659 on the dynamics of soil organic carbon decomposition in a subarctic tundra soil.
1660 *GEOSCIENCES JOURNAL*, 22(1), 121–130. <https://doi.org/10.1007/s12303-017-0052-2>
- 1661 Roehm, C. L., Giesler, R., & Karlsson, J. (2009). Bioavailability of terrestrial organic carbon to
1662 lake bacteria: The case of a degrading subarctic permafrost mire complex. *JOURNAL OF*
1663 *GEOPHYSICAL RESEARCH-BIOGEOSCIENCES*, 114.
1664 <https://doi.org/10.1029/2008JG000863>
- 1665 Rogers, J. A., Galy, V., Kellerman, A. M., Chanton, J. P., Zimov, N., & Spencer, R. G. M.
1666 (2021). Limited Presence of Permafrost Dissolved Organic Matter in the Kolyma River,
1667 Siberia Revealed by Ramped Oxidation. *JOURNAL OF GEOPHYSICAL RESEARCH-*
1668 *BIOGEOSCIENCES*, 126(7). <https://doi.org/10.1029/2020JG005977>
- 1669 Roth, V.-N., Dittmar, T., Gaupp, R., & Gleixner, G. (2013). Latitude and pH driven trends in the
1670 molecular composition of DOM across a north south transect along the Yenisei River.
1671 *Geochimica et Cosmochimica Acta*, 123, 93–105.
1672 <https://doi.org/https://doi.org/10.1016/j.gca.2013.09.002>
- 1673 Schostag, M., Stibal, M., Jacobsen, C. S., Baelum, J., Tas, N., Elberling, B., ... Prieme, A.
1674 (2015). Distinct summer and winter bacterial communities in the active layer of Svalbard
1675 permafrost revealed by DNA- and RNA-based analyses. *FRONTIERS IN*
1676 *MICROBIOLOGY*, 6. <https://doi.org/10.3389/fmicb.2015.00399>
- 1677 Shakil, S., Tank, S. E., Kokelj, S. V., Vonk, J. E., & Zolkos, S. (2020). Particulate dominance of
1678 organic carbon mobilization from thaw slumps on the Peel Plateau, NT: Quantification and
1679 implications for stream systems and permafrost carbon release. *Environmental Research*
1680 *Letters*, 15(11). <https://doi.org/10.1088/1748-9326/abac36>
- 1681 Shatilla, N. J., & Carey, S. K. (2019). Assessing inter-annual and seasonal patterns of DOC and
1682 DOM quality across a complex alpine watershed underlain by discontinuous permafrost in
1683 Yukon, Canada. *Hydrology and Earth System Sciences*, 23(9), 3571–3591.
1684 <https://doi.org/10.5194/hess-23-3571-2019>
- 1685 Shirokova, L. S., Pokrovsky, O. S., Kirpotin, S. N., Desmukh, C., Pokrovsky, B. G., Audry, S.,
1686 & Viers, J. (2013). Biogeochemistry of organic carbon, CO₂, CH₄, and trace elements in
1687 thermokarst water bodies in discontinuous permafrost zones of Western Siberia.
1688 *BIOGEOCHEMISTRY*, 113(1–3), 573–593. <https://doi.org/10.1007/s10533-012-9790-4>
- 1689 Shirokova, L. S., Bredoire, R., Rols, J.-L. L., & Pokrovsky, O. S. (2017). Moss and Peat
1690 Leachate Degradability by Heterotrophic Bacteria: The Fate of Organic Carbon and Trace
1691 Metals. *Geomicrobiology Journal*, 34(8), 641–655.
1692 <https://doi.org/10.1080/01490451.2015.1111470>
- 1693 Shirokova, L. S., Chupakov, A. V., Zabelina, S. A., Neverova, N. V., Payandi-Rolland, D.,
1694 Causserand, C., ... Pokrovsky, O. S. (2019). Humic surface waters of frozen peat bogs

- 1695 (permafrost zone) are highly resistant to bio- and photodegradation. *BIOGEOSCIENCES*,
 1696 16(12), 2511–2526. <https://doi.org/10.5194/bg-16-2511-2019>
- 1697 Shirokova, L. S., Labouret, J., Gurge, M., Gerard, E., Ivanova, I. S., Zabelina, S. A., &
 1698 Pokrovsky, O. S. (2017). Impact of Cyanobacterial Associate and Heterotrophic Bacteria on
 1699 Dissolved Organic Carbon and Metal in Moss and Peat Leachate: Application to Permafrost
 1700 Thaw in Aquatic Environments. *AQUATIC GEOCHEMISTRY*, 23(5–6), 331–358.
 1701 <https://doi.org/10.1007/s10498-017-9325-7>
- 1702 Sistla, S. A., Schaeffer, S., & Schimel, J. P. (2019). Plant community regulates decomposer
 1703 response to freezing more strongly than the rate or extent of the freezing regime.
 1704 *ECOSPHERE*, 10(2). <https://doi.org/10.1002/ecs2.2608>
- 1705 Speetjens, N. J., Tanski, G., Martin, V., Wagner, J., Richter, A., Hugelius, G., ... Vonk, J. E.
 1706 (2022). Dissolved organic matter characterization in soils and streams in a small coastal
 1707 low-arctic catchment. *Biogeosciences*, 19(July), 3073–3097. Retrieved from
 1708 <https://doi.org/10.5194/bg-19-3073-2022>
- 1709 Stutter, M. I., & Billett, M. F. (2003). Biogeochemical controls on streamwater and soil solution
 1710 chemistry in a High Arctic environment. *Geoderma*, 113(1), 127–146.
 1711 [https://doi.org/https://doi.org/10.1016/S0016-7061\(02\)00335-X](https://doi.org/https://doi.org/10.1016/S0016-7061(02)00335-X)
- 1712 Takano, S., Yamashita, Y., Tei, S., Liang, M., Shingubara, R., Morozumi, T., ... Sugimoto, A.
 1713 (2021). Stable Water Isotope Assessment of Tundra Wetland Hydrology as a Potential
 1714 Source of Arctic Riverine Dissolved Organic Carbon in the Indigirka River Lowland,
 1715 Northeastern Siberia. *Frontiers in Earth Science*, 9.
 1716 <https://doi.org/10.3389/feart.2021.699365>
- 1717 Tanski, G., Couture, N., Lantuit, H., Eulenburg, A., & Fritz, M. (2016). Eroding permafrost
 1718 coasts release low amounts of dissolved organic carbon (DOC) from ground ice into the
 1719 nearshore zone of the Arctic Ocean. *Global Biogeochemical Cycles*, 30(7), 1054–1068.
 1720 <https://doi.org/10.1002/2015GB005337>
- 1721 Tanski, G., Lantuit, H., Ruttor, S., Knoblauch, C., Radosavljevic, B., Strauss, J., ... Fritz, M.
 1722 (2017). Transformation of terrestrial organic matter along thermokarst-affected permafrost
 1723 coasts in the Arctic. *Science of the Total Environment*, 581–582, 434–447.
 1724 <https://doi.org/10.1016/j.scitotenv.2016.12.152>
- 1725 Textor, S. R., Wickland, K. P., Podgorski, D. C., Johnston, S. E., & Spencer, R. G. M. (2019).
 1726 Dissolved Organic Carbon Turnover in Permafrost-Influenced Watersheds of Interior
 1727 Alaska: Molecular Insights and the Priming Effect. *FRONTIERS IN EARTH SCIENCE*, 7.
 1728 <https://doi.org/10.3389/feart.2019.00275>
- 1729 Thompson, M. S., Giesler, R., Karlsson, J., & Klaminder, J. (2015). Size and characteristics of
 1730 the DOC pool in near-surface subarctic mire permafrost as a potential source for nearby

- 1731 freshwaters. *Arctic, Antarctic, and Alpine Research*, 47(1), 49–58.
 1732 <https://doi.org/10.1657/AAAR0014-010>
- 1733 Treat, C. C., Wollheim, W. M., Varner, R. K., & Bowden, W. B. (2016). Longer thaw seasons
 1734 increase nitrogen availability for leaching during fall in tundra soils. *ENVIRONMENTAL*
 1735 *RESEARCH LETTERS*, 11(6). <https://doi.org/10.1088/1748-9326/11/6/064013>
- 1736 Trusiak, A., Treibergs, L. A., Kling, G. W., & Cory, R. M. (2018). The role of iron and reactive
 1737 oxygen species in the production of CO₂ in arctic soil waters. *GEOCHIMICA ET*
 1738 *COSMOCHIMICA ACTA*, 224, 80–95. <https://doi.org/10.1016/j.gca.2017.12.022>
- 1739 Voigt, C., Lamprecht, R. E., Marushchak, M. E., Lind, S. E., Novakovskiy, A., Aurela, M., ...
 1740 Biasi, C. (2017). Warming of subarctic tundra increases emissions of all three important
 1741 greenhouse gases – carbon dioxide, methane, and nitrous oxide. *Global Change Biology*,
 1742 23(8), 3121–3138. <https://doi.org/10.1111/gcb.13563>
- 1743 Voigt, C., Marushchak, M. E., Mastepanov, M., Lamprecht, R. E., Christensen, T. R.,
 1744 Dorodnikov, M., ... Biasi, C. (2019). Ecosystem carbon response of an Arctic peatland to
 1745 simulated permafrost thaw. *Global Change Biology*, 25(5), 1746–1764.
 1746 <https://doi.org/10.1111/gcb.14574>
- 1747 Voigt, C., Marushchak, M. E., Lamprecht, R. E., Jackowicz-Korczyński, M., Lindgren, A.,
 1748 Mastepanov, M., ... Biasi, C. (2017). Increased nitrous oxide emissions from Arctic
 1749 peatlands after permafrost thaw. *Proceedings of the National Academy of Sciences of the*
 1750 *United States of America*, 114(24), 6238–6243. Retrieved from
 1751 <https://www.jstor.org/stable/26484198>
- 1752 Vonk, J. E., Mann, P. J., Dowdy, K. L., Davydova, A., Davydov, S. P., Zimov, N., ... Holmes,
 1753 R. M. (2013). Dissolved organic carbon loss from Yedoma permafrost amplified by ice
 1754 wedge thaw. *ENVIRONMENTAL RESEARCH LETTERS*, 8(3).
 1755 <https://doi.org/10.1088/1748-9326/8/3/035023>
- 1756 Vonk, J. E., Mann, P. J., Davydov, S., Davydova, A., Spencer, R. G. M., Schade, J., ... Holmes,
 1757 R. M. (2013). High biolability of ancient permafrost carbon upon thaw. *GEOPHYSICAL*
 1758 *RESEARCH LETTERS*, 40(11), 2689–2693. <https://doi.org/10.1002/grl.50348>
- 1759 Waldrop, M. P., Harden, J. W., Turetsky, M. R., Petersen, D. G., McGuire, A. D., Briones, M. J.
 1760 I., ... Pruetz, L. E. (2012). Bacterial and enchytraeid abundance accelerate soil carbon
 1761 turnover along a lowland vegetation gradient in interior Alaska. *Soil Biology and*
 1762 *Biochemistry*, 50, 188–198. <https://doi.org/https://doi.org/10.1016/j.soilbio.2012.02.032>
- 1763 Waldrop, M. P., & Harden, J. W. (2008). Interactive effects of wildfire and permafrost on
 1764 microbial communities and soil processes in an Alaskan black spruce forest. *GLOBAL*
 1765 *CHANGE BIOLOGY*, 14(11), 2591–2602. [https://doi.org/10.1111/j.1365-](https://doi.org/10.1111/j.1365-2486.2008.01661.x)
 1766 [2486.2008.01661.x](https://doi.org/10.1111/j.1365-2486.2008.01661.x)

- 1767 Ward, C. P., & Cory, R. M. (2015). Chemical composition of dissolved organic matter draining
1768 permafrost soils. *Geochimica et Cosmochimica Acta*, *167*, 63–79.
1769 <https://doi.org/https://doi.org/10.1016/j.gca.2015.07.001>
- 1770 Ward, C. P., Nalven, S. G., Crump, B. C., Kling, G. W., & Cory, R. M. (2017). Photochemical
1771 alteration of organic carbon draining permafrost soils shifts microbial metabolic pathways
1772 and stimulates respiration. *NATURE COMMUNICATIONS*, *8*.
1773 <https://doi.org/10.1038/s41467-017-00759-2>
- 1774 Whittinghill, K. A., Finlay, J. C., & Hobbie, S. E. (2014). Bioavailability of dissolved organic
1775 carbon across a hillslope chronosequence in the Kuparuk River region, Alaska. *Soil Biology*
1776 *and Biochemistry*, *79*, 25–33. <https://doi.org/https://doi.org/10.1016/j.soilbio.2014.08.020>
- 1777 Wickland, K. P., Neff, J. C., & Aiken, G. R. (2007). Dissolved organic carbon in Alaskan boreal
1778 forest: Sources, chemical characteristics, and biodegradability. *ECOSYSTEMS*, *10*(8),
1779 1323–1340. <https://doi.org/10.1007/s10021-007-9101-4>
- 1780 Wickland, K. P., Waldrop, M. P., Aiken, G. R., Koch, J. C., Jorgenson, Mt., & Striegl, R. G.
1781 (2018). Dissolved organic carbon and nitrogen release from boreal Holocene permafrost and
1782 seasonally frozen soils of Alaska. *ENVIRONMENTAL RESEARCH LETTERS*, *13*(6).
1783 <https://doi.org/10.1088/1748-9326/aac4ad>
- 1784 Yun, J., Jung, J. Y., Kwon, M. J., Seo, J., Nam, S., Lee, Y. K., & Kang, H. (2022). Temporal
1785 Variations Rather than Long-Term Warming Control Extracellular Enzyme Activities and
1786 Microbial Community Structures in the High Arctic Soil. *MICROBIAL ECOLOGY*, *84*(1),
1787 168–181. <https://doi.org/10.1007/s00248-021-01859-9>
- 1788 Zolkos, S., & Tank, S. E. (2019). *Permafrost geochemistry and retrogressive thaw slump*
1789 *morphology (Peel Plateau, Canada), v. 1.0 (2017-2017)*. [https://doi.org/10.5885/45573XD-](https://doi.org/10.5885/45573XD-28DD57D553F14BF0)
1790 [28DD57D553F14BF0](https://doi.org/10.5885/45573XD-28DD57D553F14BF0)
- 1791